IEEE Access
Multidisciplinary ⋮ Rapid Review ⋮ Open Access Journal

Received September 16, 2019, accepted October 9, 2019, date of publication October 22, 2019, date of current version November 1, 2019.

Digital Object Identifier 10.1109/ACCESS.2019.2948970

Protograph-Based Globally-Coupled LDPC Codes Over the Gaussian Channel With Burst Erasures

JI ZHANG[1,2], BAOMING BAI[1], (Senior Member, IEEE), MIN ZHU[1], (Member, IEEE), SHUANGYANG LI[1], (Student Member, IEEE), AND HUAAN LI[1]

[1]State Key Laboratory of Integrated Service Networks, Xidian University, Xi'an 710071, China
[2]School of Mathematics and Statistics, Henan University of Science and Technology, Luoyang 471000, China

Corresponding authors: Baoming Bai (bmbai@mail.xidian.edu.cn) and Min Zhu (zhunanzhumin@gmail.com)

This work was supported in part by the National Natural Science Foundation of China under Grant 61771364 and Grant 61701368, in part by the Key Research and Development Project of Guangdong Province under Grant 2018B010114001, in part by the Key Research and Development Project of Shaanxi Province under Grant 2018ZDCXL-GY-04-05, in part by the Innovation Fund of Xidian University under Grant JB182001, and in part by the Youth Foundation of the Henan University of Science and Technology under Grant 2014QN030.

ABSTRACT This paper presents two types of protograph-based globally-coupled low-density parity-check (GC-LDPC) codes formed by a new edge spreading operation. This operation is called the *global edge spreading*. The Gaussian approximation (GA) and the protograph-based extrinsic information transfer (P-EXIT) analysis are then generalized over a special type of burst-erasure channels (BuECs). Such channel incorporates both Gaussian noise and burst erasures, and is denoted by the Gaussian channel with burst erasures (BuEC-G). Furthermore, the stability condition for BuECs-G is proved and an edge spreading optimization method is proposed to design the structured GC-LDPC codes by predicting the iterative decoding thresholds of corresponding protographs. Simulation results show that the optimized GC-LDPC codes can achieve better thresholds and error performances than existing well-designed GC-LDPC codes, and provide near-capacity performances over BuECs-G.

INDEX TERMS Globally-coupled low-density parity-check codes, Gaussian approximation, protograph-based extrinsic information transfer, burst-erasure, Gilbert-Elliott erasure.

I. INTRODUCTION

For the data transmission, data packets are inevitably influenced by both random noise and interference (burst-noise). Usually, the random noise is a white Gaussian process, while the burst-noise is approximated by the specific noise with deterministic characteristics, such as erasure [1], impulse noise [2], and the bursty noise [3]. In this paper, we focus on a special burst-erasure channel (BuEC) which incorporates both random noise (Gaussian noise) and erasures. Taking the magnetic (or optical) recording system as an example, we can regard its background noise as the white Gaussian noise, and designate the detected thermal asperities (or scratches) at the decoder as erasures [4], [5]. The noise in such channel is the combination of the background Gaussian noise and erasures, this is different from the classic erasure-burst channel (defined in [1]) that only considers erasures. So, we refer to this type of channels as the *Gaussian channel with burst erasures* (BuEC-G) [6]. J. Ha *et al.* introduced a mixed channel model for the BuEC-G in [4] and proposed a method for optimizing degree distributions of low-density parity check (LDPC) codes based on the Gaussian approximation (GA) analysis [4], [7], [8]. With respect to such channel model, outputs are randomly erased with a small erasure probability rather than dropped in a bursty fashion. K. Li *et al.* presented a new type of BuECs-G in [5]. They regarded the channel as a concatenation of a memoryless channel (or an indecomposable finite-state channel) and a burst-erasure channel, and derived the non-feedback capacity of this channel. Note that the burst-erasure in this channel is assumed as consecutive erasures with fixed length. However, in practical systems, the occurrence time and the duration of burst-noise are usually variable. Therefore, L. Song *et al.* proposed a new type of BuECs-G by changing these consecutive erasures to a single erasure process with an explicit input-output functional relationship [9]. The feedback and non-feedback capacities of such channels were discussed, respectively. At present, the existing coding techniques for the

The associate editor coordinating the review of this manuscript and approving it for publication was Rui Wang.

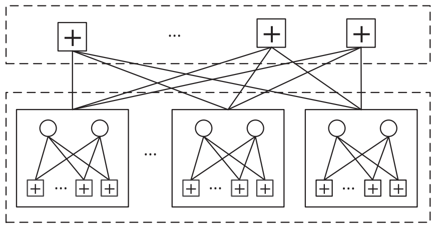

FIGURE 1. **The Tanner graph of GC-LDPC code.**

classic erasure-burst channel have been extensively studied in [10]–[13]. However, there are not many works addressing the construction of coding schemes over the BuEC-G with finite-state erasure process [14]–[20]. Thus, the main motivation of this paper is to study the coding techniques for such channels.

LDPC codes are a type of error-correcting codes which have shown excellent performance over binary erasure channels (BECs) [21]. There are two ways to reduce the impact of the burst-erasure noise on LDPC codes. The first way is to employ the concatenated structure (such as using the maximum distance separable (MDS) codes as the outer codes and LDPC codes as the inner codes) to mitigate the burst erasures noise. However, the concatenated structure would increase decoding complexity and delay. The other way focuses on constructing and optimizing the parity-check matrices of LDPC codes with good error-correction capabilities and large maximum resolvable erasure burst length [4], [5], [11], [12], [22]. The algebraic construction is one of the important design methods for combating the burst erasures noise. In 2016, Li *et al.* [22] introduced a class of algebraic LDPC codes which are capable of correcting erasures clustered in burst with low latency. Since such LDPC codes are designed for improving the reliability and the convergence speed of the iterative decoder by adding some additional check nodes (called the *global* check nodes, global CNs) to link a set of small disjoint Tanner graphs of LDPC codes (called the *local* part) together (as shown in Fig. 1), we refer to these type of LDPC codes as globally-coupled LDPC (GC-LDPC) codes [22]–[30]. Currently, the design of the GC-LDPC code is mainly based on finite fields, and the error performances of the existing GC-LDPC codes are closely related to the selection of parameters (such as the size of the circulant permutation matrix (CPM), the number of the *global* CNs and the sizes of the *local* parts). However, most existing works only provided a preliminary analysis of the decoding performance of GC-LDPC codes through performance simulations while approaches of how to select these parameters and decoding convergence analysis of the iterative decoders are seldom mentioned. Therefore, it is necessary to find some effective methods to design GC-LDPC codes.

The aim of this paper is to study a class of GC-LDPC codes to combat the Gaussian noise and erasures. We first introduce the BuEC-G whose erasure rate and erasure duration are determined by a random or Gilbert-Elliott erasure model. For the decoding process, the log-likelihood ratios (LLRs) of channel outputs tend to zero when erasure occurs. Thus we can view the erasure noise as some interferences that eliminate the information from the channel, and then evaluate thresholds of the iterative decoding by the extrinsic information transfer (EXIT) analysis [10], [32]–[34]. On the other hand, a major difficulty of designing GC-LDPC codes is to determine the relationship between the structure of GC-LDPC codes and the threshold of iterative decoding over BuECs-G [35], [36]. In order to facilitate the analysis and design, we propose a new edge spreading technique to construct the protograph-based GC-LDPC codes and such technique is referred to as the "global edge spreading". Different from the existing edge spreading technique [36], the proposed technique spreads the edges which are emanating from the local CNs to some specific global CNs. Furthermore, we generalize the GA and protograph-based EXIT (P-EXIT) analysis to the BuEC-G for calculating convergence thresholds of the iterative decoding, and present an edge spreading optimization method to minimize the gap between the capacity and the iterative decoding threshold of GC-LDPC codes over BuECs-G.

The main contributions of this paper are summarized as follows.

- We present a new type of edge spreading operation, called *global edge spreading* operation. Using such operation, we propose two types of protograph-based GC-LDPC codes.
- We discuss the GA and the stability condition over BuECs-G and generalize the P-EXIT analysis to the BuEC-G.
- Based on the GA and P-EXIT analysis, we present an edge spreading optimization method for minimizing the gap between the capacity and the iterative decoding threshold of GC-LDPC codes for a given range of code rates and code lengths over BuECs-G. Numerical results show that the proposed globally-coupled quasi-cyclic LDPC (GC-QC-LDPC) codes can achieve better thresholds and error performance compared to the existing well-designed GC-QC-LDPC codes over additive white Gaussian noise (AWGN) channels and BuECs-G.

The remainder of this paper is organized as follows. In Section II, we describe the BuEC-G. Section III gives a brief introduction of GC-LDPC codes and introduces the *global edge spreading* operation for forming the protograph-based GC-LDPC code. In Section IV, we analyze the decoding threshold of GC-LDPC codes by the GA and the P-EXIT. Section V presents the edge spreading optimization method for designing the GC-QC-LDPC codes and shows the numerical results for the proposed GC-LDPC codes. Section VI concludes this paper.

Notation: We use lowercase letters (e.g. x) to denote scalars, bold lowercase letter (e.g. $\mathbf{x}$) to denote vectors, boldface capital letters (e.g. $\mathbf{X}$) for matrices, and bold uppercase letter (e.g. X) to denote the set of the nodes or edges in bipartite graph. We denote by b_{ij} the element in the ith row and jth column of a matrix $\mathbf{B}$. The notation $\mathbb{E}[\cdot]$ stands for

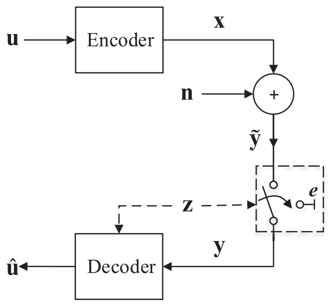

(a) System configuration

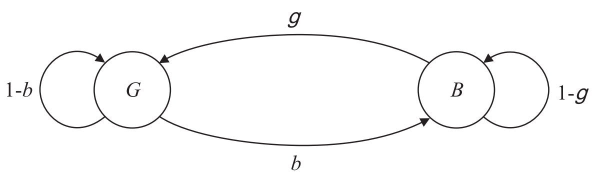

(b) Gilbert-Elliott erasure model

FIGURE 2. Channel model for the BuEC-G.

expectation. The superscript "(pt)" and "T" stand for protograph and transpose, respectively, and the subscripts "lp" and "gp" stand for *local part* and *global part*, respectively. We use calligraphic font $\mathcal{C}$ to denote the GC-LDPC code and list some special notations used in this paper as follows:

- $K_{\text{GA/P-EXIT}}$: Bit signal-to-noise ratio (SNR) threshold computed by GA/P-EXIT.
- $W_{\text{GA/P-EXIT}}$: Metric value of the iterative decoding threshold of GC-LDPC codes over BuECs-G computed by GA/P-EXIT.

II. THE CHANNEL MODEL FOR THE BUEC-G

In this section, we briefly introduce the BuEC-G model under consideration. The corresponding system configuration is depicted in Fig. 2(a). Let $\mathbf{u} = [u_0, u_1, \ldots, u_{K-1}]$ be the binary information sequence of length K and $\mathbf{x} = [x_0, x_1, \ldots, x_{N-1}]$ be the corresponding coded sequence of length N, where $x_i \in \{\pm 1\}$. Suppose that $\mathbf{x}$ is transmitted over the AWGN channel, resulting in the output sequence $\tilde{\mathbf{y}} = [\tilde{y}_0, \tilde{y}_1, \ldots, \tilde{y}_{N-1}]$, where $\tilde{y}_i = x_i + n_i$ with n_i being independent Gaussian noise samples with zero mean and variance σ^2. At the receiver side, $\tilde{\mathbf{y}}$ is assumed to be pre-processed, i.e., the less reliable symbols are erased. This can equivalently be thought that $\tilde{\mathbf{y}}$ is passed through an erasure channel. If a transmission symbol is erased, we replace such symbol by "e". Let $\mathbf{y} = [y_0, y_1, \ldots, y_{N-1}]$ be the input sequence to the decoder, and $\mathbf{z} = [z_0, z_1, \ldots, z_{N-1}]$ with $z_i \in \{0, 1\}$ be the erasure indication sequence, where $z_i = 1$ indicates the erasing of $\tilde{y}_i$. As a result, the relationship for the BuEC-G can be expressed as

$$y_i = \begin{cases} x_i + n_i, & \text{if } z_i = 0, \\ e, & \text{if } z_i = 1. \end{cases}$$

where $0 \le i \le N-1$.

When $\{z_i\}$ are independent and identically distributed, the mixed channel model becomes a mixture of the Gaussian channel with random erasure (called REC-G) as mentioned in [4]. If the sequence $\mathbf{z}$ is generated by using a Gilbert-Elliott model, the mixed channel model becomes a mixture of the Gaussian channel with Gilbert-Elliott erasure (called GEC-G). As shown in Fig. 2(b), the Gilbert-Elliott model is a Markov chain with two states "G" and "B", where "G" represents the good state, and "B" represents the bad state. The erasure process is independent from the channel input and depends on a state process $\{s_i\}_{i=0}^{\infty}$, $s_i \in \{G, B\}$. Assume that in states "G" and "B" erasures ($z_i = 1$) are generated with probability $\varepsilon_G \triangleq \Pr\{z_i = 1|s_i = G\}$ and $\varepsilon_B \triangleq \Pr\{z_i = 1|s_i = B\}$, respectively. We denote the transition probabilities by $g \triangleq \Pr\{s_{i+1} = G|s_i = B\}$ and $b \triangleq \Pr\{s_{i+1} = B|s_i = G\}$, respectively. The initial distributions of the state process are assumed to be $\pi_G = \Pr\{s_0 = G\} = g/(g+b)$, $\pi_B = \Pr\{s_0 = B\} = b/(g+b)$, which ensure its stationarity. Let ε_{GB} be the total erasure probability over the Gilbert-Elliott channel in the steady-state. Then, we have $\varepsilon_{GB} = \Pr\{z_i = 1\} = \varepsilon_G\pi_G + \varepsilon_B\pi_B$.

Since the erasure duration follows a geometric distribution [15], the average burst length of the state "B" is $\triangle_B = \sum_i i(1-g)^{i-1}g = 1/g$. So, we have

$$\begin{cases} b = \dfrac{\varepsilon_{GB} - \varepsilon_G}{\triangle_B(\varepsilon_B - \varepsilon_{GB})}, & \text{for } \varepsilon_B \neq \varepsilon_{GB}, \\ g = \dfrac{1}{\triangle_B}. \end{cases}$$

Note that, $b(\varepsilon_{GB}, \triangle_B)$ is monotone increasing for $\varepsilon_{GB} < \varepsilon_B$ with a fixed $\triangle_B$. We have

$$0 \le \varepsilon_{GB} \le \frac{\triangle_B\varepsilon_B - 2\varepsilon_G}{2 + \triangle_B},$$

and

$$\triangle_B \ge \max\left\{2, \left\lceil \frac{\varepsilon_{GB} - \varepsilon_G}{2(\varepsilon_B - \varepsilon_{GB})} \right\rceil\right\}.$$

The probability of runs of zeros [15] is defined by (1), as shown at the bottom of the next page. In [15] a recurrence formula for $U(j)$ is given by

$$\begin{aligned} U(j) = {} & [(1-b)(1-\varepsilon_G) + (1-g)(1-\varepsilon_B)]U(j-1) \\ & + (1-\varepsilon_B)(1-\varepsilon_G)(g+b-1)U(j-2), \end{aligned}$$

for $j \in \{2, 3, \ldots\}$. Initial values are $U(0) = 1$,

$$\begin{aligned} U(1) = {} & \frac{g\varepsilon_G\Big(b(1-\varepsilon_B) + (1-b)(1-\varepsilon_G)\Big)}{(g\varepsilon_G + b\varepsilon_B)} \\ & + \frac{b\varepsilon_B\Big(g(1-\varepsilon_G) + (1-g)(1-\varepsilon_B)\Big)}{(g\varepsilon_G + b\varepsilon_B)}. \end{aligned}$$

The average erasure rate in the Gilbert-Elliott model is given by

$$\varepsilon_{ch} = \frac{1}{N}\sum_{i=0}^{N-1}\Pr\{z_i = 1\} = \frac{1}{N}\sum_{i=0}^{N-1}\sum_{j=0}^{i-1}\left(1 - \frac{U(j+1)}{U(j)}\right). \quad (2)$$

For $\varepsilon_G = 0$, we give an estimate of the values of ε_{ch} over the Gilbert-Elliott channel as follows:

$$\begin{aligned}\varepsilon_{ch}(\varepsilon_{GB}, g, b) &\approx \frac{1}{N}\sum_{i=0}^{N-1} \Pr\{z_i = 1|z_0 = 1\} \\ &= \frac{1}{N}\sum_{i=0}^{N-1} \frac{\Pr\{z_i = 1, z_0 = 1\}}{\varepsilon_{GB}} \\ &= \hat{\varepsilon}_{ch}(\varepsilon_{GB}, g, b), \end{aligned} \quad (3)$$

where

$$\hat{\varepsilon}_{ch}(\varepsilon_{GB}, g, b) = \begin{cases} 0, & \text{if } \varepsilon_{GB} = 0, \\ \frac{1}{N}(1 + \sum_{i=1}^{N-1} \varepsilon_{GB}[1 + \frac{g}{b}(1-b-g)^i]), & \text{otherwise.} \end{cases}$$

Theorem 1: The capacity for the GEC-G described above is given by

$$C_{GEC-G} = (1 - \varepsilon_{ch}) C_{AWGN},$$

where C_{AWGN} is the capacity for the AWGN channel.

We give its sketch in the Appendix.

III. GLOBALLY-COUPLED LDPC CODES

In this section, we first briefly review the construction methods of two types of GC-LDPC codes and introduce two types of the protograph-based GC-LDPC codes.

A. CONSTRUCTION OF GC-LDPC CODES: CASCADED TYPE

We begin with the first type called cascaded type GC-LDPC code. For this type of GC-LDPC codes, we construct a base matrix $\mathbf{B}_W$ over GF(q) of size $rk \times rk$, such as

$$\mathbf{B}_W = \begin{bmatrix} \alpha^0 - 1 & \alpha - 1 & \cdots & \alpha^{q-2} - 1 \\ \alpha^{q-2} - 1 & \alpha^0 - 1 & \cdots & \alpha^{q-3} - 1 \\ \vdots & \vdots & \ddots & \vdots \\ \alpha - 1 & \alpha^2 - 1 & \cdots & \alpha^0 - 1 \end{bmatrix}, \quad (4)$$

where α is a primitive element of GF(q), r and k are two integers satisfying $rk = q-1$. Partition $\mathbf{B}_W$ into the following $r \times r$ array:

$$\begin{bmatrix} \mathbf{W}_{00} & \mathbf{W}_{01} & \cdots & \mathbf{W}_{0(r-1)} \\ \mathbf{W}_{10} & \mathbf{W}_{11} & \cdots & \mathbf{W}_{1(r-1)} \\ \vdots & \vdots & \ddots & \vdots \\ \mathbf{W}_{(r-1)0} & \mathbf{W}_{(r-1)1} & \cdots & \mathbf{W}_{(r-1)(r-1)} \end{bmatrix},$$

where $\mathbf{W}_{ij}$ are $k \times k$ matrices.

By removing the last $k - n$ columns of $\mathbf{W}_{ij}$, we obtain an $r \times r$ array $\mathbf{B}_V$ of $k \times n$ submatrices. Keep m rows of each submatrix of $\mathbf{B}_V$ and obtain the following $r \times r$ array:

$$\widetilde{\mathbf{B}}_V = \begin{bmatrix} \mathbf{B}_{00} & \mathbf{B}_{01} & \cdots & \mathbf{B}_{0(r-1)} \\ \mathbf{B}_{10} & \mathbf{B}_{11} & \cdots & \mathbf{B}_{1(r-1)} \\ \vdots & \vdots & \ddots & \vdots \\ \mathbf{B}_{(r-1)0} & \mathbf{B}_{(r-1)1} & \cdots & \mathbf{B}_{(r-1)(r-1)} \end{bmatrix}.$$

Extract a $t \times t$ array from the top left corner of $\widetilde{\mathbf{B}}_V$ to form $\mathbf{B}_R = [\mathbf{B}_{ij}]_{0 \le i,j \le t-1}$, where $t \le r$. Then take s unused rows of $\mathbf{B}_V$ to obtain an $s \times nt$ matrix $\mathbf{B}_X$. Thus, we have the following base matrix of GC-QC-LDPC codes:

$$\begin{aligned}\mathbf{B}_{gc,1} &= [b_{ij}]_{0 \le i < mt+s, 0 \le j < nt} \\ &= \mathbf{B}_R \circ \{\mathbf{I}_t \otimes \mathbf{E}\} \oplus \mathbf{B}_X \\ &= \left[\begin{array}{cccc} \mathbf{B}_{00} & & & \\ & \mathbf{B}_{11} & & \\ & & \ddots & \\ & & & \mathbf{B}_{(t-1)(t-1)} \\ \hdashline & \mathbf{B}_X & & \end{array}\right],\end{aligned}$$

where "$\circ$" denotes the Hadamard product [37] (i.e., entry-wise product of two matrices), "$\oplus$" denotes the direct-sum[1] [38, Chapter 4], "$\otimes$" denotes the Kronecker product, $\mathbf{I}_t$ is a t-dimensional identity matrix, and $\mathbf{E}$ is an $m \times n$ all-one matrix.

For each entry in $\mathbf{B}_{gc,1}$, if b_{ij} is the zero element of GF(q), then replace b_{ij} by the $(q-1) \times (q-1)$ zero matrix (ZM), and if $b_{ij} = \alpha^k$ with $0 \le k < q-1$, then replace b_{ij} by a $(q-1) \times (q-1)$ CPM whose first row has a single 1-component at the kth element. This operation is referred to as the $(q-1)$-fold dispersion of $\mathbf{B}_{gc,1}$, which will result in an $(mt+s) \times nt$ array $\mathbf{H}_{gc,1}$ of $(q-1) \times (q-1)$ CPMs and/or ZMs. The null space of $\mathbf{H}_{gc,1}$ gives a GC-QC-LDPC code whose Tanner graph has a girth of at least 6, denoted by $\mathcal{C}_{cas}$.

B. CONSTRUCTION OF GC-LDPC CODES: INTERLEAVED TYPE

Based on the base matrix $\mathbf{B}_W$ in (4), we can form another type of GC-LDPC codes. Let l, t, and f be three positive integers satisfying $2ltf < rk$. First, we obtain an $rk \times 2ltf$ matrix $\mathbf{B}_V$ by removing the last $rk - 2ltf$ columns from $\mathbf{B}_W$. Take the first tf rows from $\mathbf{B}_V$ to obtain a $tf \times 2ltf$ matrix $\widetilde{\mathbf{B}}_V$ and divide each row into $2tl$ sections, each consisting of f components. Thus, there are t sectionalized rows. Denote the ith sectionalized row of $\widetilde{\mathbf{B}}_V$ as $\widetilde{\mathbf{B}}_i$, where $0 \le i \le t-1$.

[1]Here, we use the definition of *direct-sum* in [38], i.e., $\mathbf{M}_1 \oplus \mathbf{M}_2 = [\mathbf{M}_1 \mathbf{M}_2]^T$, where $\mathbf{M}_1$ and $\mathbf{M}_2$ are two matrices with the same number of columns.

$$\begin{aligned}U(j) &= \Pr\{z_{i+1} = \cdots = z_{i+j} = 0|z_i = 1\} \\ &= \Pr\{s_i = B|z_i = 1\} \cdot \Pr\{z_{i+1} = \cdots = z_{i+j} = 0|s_i = B\} \\ &\quad + \Pr\{s_i = G|z_i = 1\} \cdot \Pr\{z_{i+1} = \cdots = z_{i+j} = 0|s_i = G\}, \quad \text{for} \quad i \in \{0, 1, \ldots, N-1\} \end{aligned} \quad (1)$$

Subsequently, we form t masking matrices of size $f \times 2ltf$, denoted by $\mathbf{M}_i$, $0 \le i \le t-1$. Divide each row of $\mathbf{M}_i$ into $2tl$ sections, each containing f components. For $0 \le j \le l-1$, the $(i+2tj)$th section of $\mathbf{M}_i$ is an $f \times f$ lower triangular matrix $\mathbf{M}_{low}$ all of whose entries on and below the main diagonal are unit elements. The $(i+2tj+t)$th section of $\mathbf{M}_i$ is an $f \times f$ upper triangular matrix $\mathbf{M}_{up}$ all of whose entries on and above the main diagonal are unit elements, and the rest sections of $\mathbf{M}_i$ are composed of some all-zero matrices. Thus, we have

$$\mathbf{M}_i = \Big[\overbrace{\mathbf{M}_i^\star \cdots \mathbf{M}_i^\star}^{l}\Big],$$

where $\mathbf{M}_i^\star = \Big[\overbrace{\mathbf{O}\cdots\mathbf{O}}^{i}\,\mathbf{M}_{low}\,\overbrace{\mathbf{O}\cdots\mathbf{O}}^{t-i-1}\,\mathbf{M}_{up}\,\overbrace{\mathbf{O}\cdots\mathbf{O}}^{t-1}\Big]$ and $\mathbf{O}$ is an $f \times f$ all-zero matrix. For $0 \le i \le t-1$, we can construct an $f \times 2ltf$ matrix $\mathbf{B}_i$ by masking $\widetilde{\mathbf{B}}_i$ with $\mathbf{M}_i$, i.e., $\mathbf{B}_i = \widetilde{\mathbf{B}}_i \circ \mathbf{M}_i$.

Take s unused rows from the rest $(rk - tf)$ rows from $\mathbf{B}_V$ to form an $s \times nt$ matrix $\mathbf{B}_X$. Then, we have the following base matrix of GC-QC-LDPC codes:

$$\begin{aligned}\mathbf{B}_{gc,2} &= \mathbf{B}_0 \oplus \mathbf{B}_1 \oplus \cdots \oplus \mathbf{B}_{t-1} \oplus \mathbf{B}_X \\ &= [\mathbf{B}_0\ \mathbf{B}_1 \cdots \mathbf{B}_{t-1}\ \mathbf{B}_X]^T.\end{aligned}$$

The $(q-1)$-fold dispersion of $\mathbf{B}_{gc,2}$ results in an $(ft+s) \times 2lft$ array $\mathbf{H}_{gc,2}$ of $(q-1)\times(q-1)$ CPMs and/or ZMs. The null space of $\mathbf{H}_{gc,2}$ gives a GC-QC-LDPC code whose Tanner graph has a girth of at least 6, denoted by $\mathcal{C}_{inter}$.

C. DEFINITION OF GLOBAL EDGE SPREADING

In this subsection, we introduce a definition of the operation on protograph which allows us to obtain a globally-coupled protograph from a block protograph.

A protograph (V, C, E) can be viewed as a small bipartite graph which consists of a set of n_v VNs $V = \{v_0, \ldots, v_{n_v-1}\}$, a set of n_c CNs $C = \{c_0, \ldots, c_{n_c-1}\}$, and a set of edges E, respectively. Let F be a positive integer. By taking an *F-fold graph cover* (see [35], [36]) or "*F-(lifting)*" of (V, C, E), we obtain a Tanner graph of a protograph-based LDPC code of block length $N = Fn_v$.

The protograph can be represented by its $n_c \times n_v$ base biadjacency matrix $\mathbf{B}^{(pt)} = [b_{ij}^{(pt)}]$, where $0 \le i < n_c$ and $0 \le j < n_v$. We refer to this base biadjacency matrix as the *protomatrix* [44]. The entry $b_{ij}^{(pt)}$ denotes the number of edges connecting VN v_j to CN c_i. By replacing each non-zero entry in $\mathbf{B}^{(pt)}$ with a sum of $b_{ij}^{(pt)}$ permutation matrices of size $F \times F$ and each zero entry with the $F \times F$ all-zero matrix, we obtain the parity-check matrix $\mathbf{H}$ of size $Fn_c \times Fn_v$ for a protograph-based LDPC code.

Definition 1 (Global Edge Spreading): Consider replicating a block protograph with b_v VNs and b_c CNs as a sequence of disjoint graphs. Suppose the VN v_j is connected to the CN c_i by $b_{ij}^{(pt)}$ edges in each protograph, where $0 \le i \le b_c-1$, and $0 \le j \le b_v-1$. Then, the VN v_j *spreads* (connects) the $b_{gp,kj}^{(pt)}$ edges from the CN c_i to the new CN $c_{gp,k}$ (global CNs), where $0 \le k \le b_g-1$ and b_g is the number of global CNs. It means that there are $\sum_{i=0}^{b_c-1} b_{lp,ij}^{(pt)} = \sum_{i=0}^{b_c-1} b_{ij}^{(pt)} - \sum_{k=0}^{b_g-1} b_{gp,kj}^{(pt)}$ edges remaining to connect to local CNs from v_j, where $b_{gp,kj}^{(pt)}$ denotes the number of edges connecting the VN v_j to the local CN $c_{lp,i}$. By repeating this operation for every b_v VNs, we obtain a globally-coupled protograph.

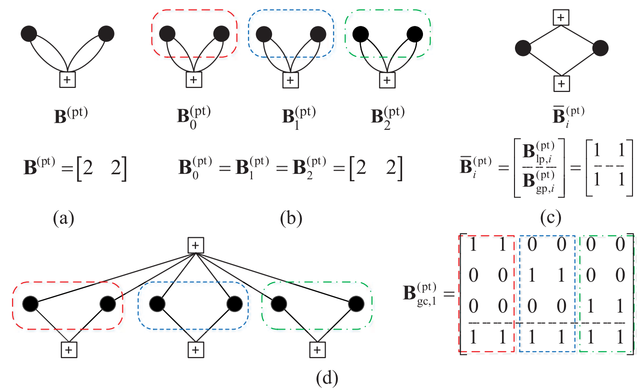

FIGURE 3. (a) Protograph representing a (2, 4)-regular LDPC-BC ensemble, (b) replicated (2, 4)-regular LDPC-BC protographs, (c) illustration of global edge spreading operation for one segment of the graph, and (d) protograph representing a (globally-coupled) GC-LDPC ensemble.

For the global edge spreading operation, if all edges emanating from each VN are connected to new (global) CNs, we have $\sum_{i=0}^{b_c-1} b_{ij}^{(pt)} = \sum_{k=0}^{b_g-1} b_{gp,kj}^{(pt)}$ for $0 \le j \le b_v - 1$. We refer to such operation as the *all-edge spreading*. Furthermore, for the *all-edge spreading* operation, if all the edges emanating from each VN are connected to new (global) CNs with the same connection pattern of the original edges, we have $b_{ij}^{(pt)} = b_{gp,ij}^{(pt)}$, where $0 \le i \le b_c - 1$ and $0 \le j \le b_v - 1$. Such operation is referred to as the *all-edge uniform spreading*.

D. CONSTRUCTION OF PROTOGRAPH-BASED GC-LDPC CODES

In this subsection, we introduce two types of the protograph-based GC-LDPC codes. These protographs are obtained by connecting or *global coupling* a sequence of disjoint protographs together.

As shown in Fig. 3(a), we have a $(d_v = 2, d_c = 4)$-regular (block) protograph with the design rate $R_d = 1 - d_v/d_c = 1/2$, where d_v and d_c denote the degrees of VNs and CNs, respectively. Let $\mathbf{B}^{(pt)}$ be an $m \times n$ protomatrix of such protograph. Here, $m = 1$, $n = 2$, and $\mathbf{B}^{(pt)} = [2\ \ 2]$.

Put t copies $(t = 3)$ of such (d_v, d_c)-regular protograph together to obtain a sequence of non-interacting graphs whose corresponding protomatrix is a 3×3 array $\widetilde{\mathbf{B}}^{(pt)}$ as follows:

$$\widetilde{\mathbf{B}}^{(pt)} = \begin{bmatrix} \mathbf{B}_0^{(pt)} & & \\ & \mathbf{B}_1^{(pt)} & \\ & & \mathbf{B}_2^{(pt)} \end{bmatrix},$$

where $\mathbf{B}_0^{(pt)} = \mathbf{B}_1^{(pt)} = \mathbf{B}_2^{(pt)} = \mathbf{B}^{(pt)} = [2\ \ 2]$, *cf.* Fig. 3(b). A global edge spreading operation applied to a VN is shown in Fig. 3(c). The edges of each VN are spread from the local CNs to the new CNs (global CNs). We can observe that there is exactly one edge, which emanates from each VN, spreading (connecting) to the "top" (the global CN). From the perspective of protomatrix, the global edge spreading rule assigns the edge associated with each VN in $\mathbf{B}_i^{(pt)}$ to $\mathbf{B}_{gp,i}^{(pt)}$ and $\mathbf{B}_{lp,i}^{(pt)}$, $0 \le i \le t-1$. Thus, the protomatrices corresponding to this global edge spreading are

$$\overline{\mathbf{B}}_i^{(pt)} = \begin{bmatrix} \mathbf{B}_{lp,i}^{(pt)} \\ \hdashline \mathbf{B}_{lp,i}^{(pt)} \end{bmatrix} = \begin{bmatrix} 1 & 1 \\ \hdashline 1 & 1 \end{bmatrix}.$$

As shown in Fig. 3(d), such global edge spreading is applied to each VN, resulting in a GC-LDPC ensemble. We refer to such GC-LDPC ensembles as the *type-1 GC-LDPC ensembles*. The protomatrix corresponding to the type-1 globally-coupled protograph of Fig. 3(d) is

$$\mathbf{B}_{gc,1}^{(pt)} = \begin{bmatrix} \mathbf{B}_{lp,0}^{(pt)} & & & \\ & \mathbf{B}_{lp,1}^{(pt)} & & \\ & & \ddots & \\ & & & \mathbf{B}_{lp,t-1}^{(pt)} \\ \hdashline \mathbf{B}_{gp,0}^{(pt)} & \mathbf{B}_{gp,1}^{(pt)} & \cdots & \mathbf{B}_{gp,t-1}^{(pt)} \end{bmatrix},$$

where $\mathbf{B}_{lp,i}^{(pt)}$ and $\mathbf{B}_{gp,i}^{(pt)}$ are $m \times n$ and $s \times n$ protomatrices, respectively, for $0 \le i \le t-1$. The protomatrix $\mathbf{B}_{lp,i}^{(pt)}$ represents the edge connections from the n VNs to the m local CNs at ith section. Similarly, the protomatrix $\mathbf{B}_{gp,i}^{(pt)}$ represents the edge connections from the n VNs to the s global CNs at ith section.

Let R_d be the design rate of the protograph-based LDPC ensemble, and n_{tr} be the number of transmitted VNs in the protograph. For the type-1 protograph-based GC-LDPC ensemble, we have

$$R_d = \frac{n_v - n_c}{n_{tr}} = \frac{nt - (mt + s)}{n_{tr}}.$$

Note that, in the case of $n_{tr} = n_v = nt$ (there is no puncture) the design rate is equal to $1 - m/n - s/nt$. Thus, the design rate of the case shown in Fig. 3 is $R_d = 1 - m/n - s/nt = 1/3$, where $m = 1$, $n = 2$, $s = 1$, and $t = 3$.

Fig. 4 illustrates the global edge spreading operation applied to two irregular protographs with protomatrices $\mathbf{B}_{low}^{(pt)}$ and $\mathbf{B}_{up}^{(pt)}$. We prefer the expression of these protomatrices as follows:

$$\mathbf{B}_{low}^{(pt)} = [b_{ij}^{(pt)}]_{0 \le i,j \le f-1} = [\mathbf{B}_{up}^{(pt)}]^T,$$

where

$$b_{ij}^{(pt)} = \begin{cases} 1 + s, & \text{if } i = j \text{ and } s \ge 1, \\ 1, & \text{if } i < j, \\ 0, & \text{otherwise.} \end{cases}$$

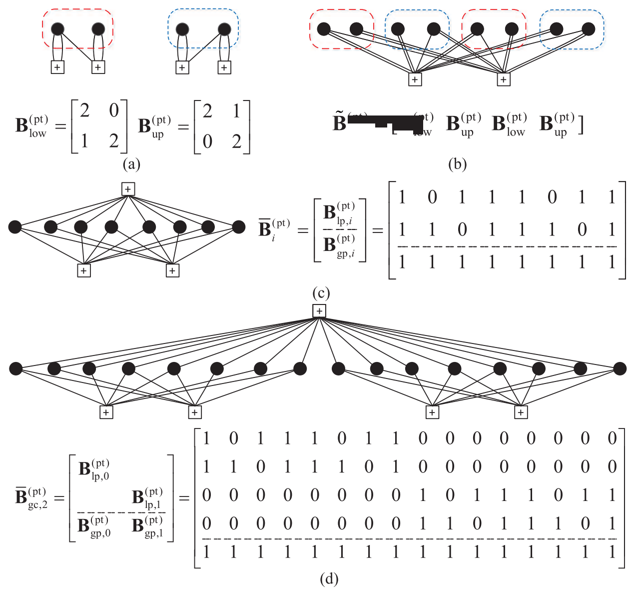

FIGURE 4. **(a) Protograph representing two irregular LDPC-BC ensembles, (b) the all-edge uniform spreading operation on each VN of the replicating the pair of irregular protographs, (c) illustration of the global edge spreading operation for one segment of the graph, and (d) protograph representing a GC-LDPC ensemble without interleaving.**

Thus, we have

$$\mathbf{B}_{low}^{(pt)} = [\mathbf{B}_{up}^{(pt)}]^T = \begin{bmatrix} s+1 & 0 & \cdots & 0 \\ 1 & s+1 & \ddots & \vdots \\ \vdots & \ddots & \ddots & 0 \\ 1 & \cdots & 1 & s+1 \end{bmatrix}_{f \times f}.$$

These two irregular protographs with $f = 2$ are shown in Fig. 4(a).

Next, we replicate the pair of such irregular protographs as l subgraphs and use the *all-edge uniform spreading* operation to each VN of these subgraphs, whose corresponding protomatrix is the following $f \times 2lf$ matrix $\widetilde{\mathbf{B}}^{(pt)}$:

$$\widetilde{\mathbf{B}}^{(pt)} = \begin{bmatrix} \mathbf{B}_{low}^{(pt)} & \mathbf{B}_{up}^{(pt)} & \cdots & \mathbf{B}_{low}^{(pt)} & \mathbf{B}_{up}^{(pt)} \end{bmatrix}_{f \times 2lf},$$

cf. Fig. 4(b). It is important to point out that the new (global) CNs, which are obtained from the *all-edge uniform spreading* operation, are treated as the local CNs in the following operations. Subsequently, we replicate the corresponding protograph of $\widetilde{\mathbf{B}}^{(pt)}$ as t disjoint graphs ($t = 2$ in Fig. 4(c)). Starting from $\widetilde{\mathbf{B}}^{(pt)}$, the global edge spreading rule assigns the edge associated with each VN in $\widetilde{\mathbf{B}}_i^{(pt)}$ to $\mathbf{B}_{gp,i}^{(pt)}$ and $\mathbf{B}_{lp,i}^{(pt)}$ for $0 \le i \le t-1$. Note that the global edge spreading operation "resolve" the parallel edges emanating from each VN in the protograph, as shown in Fig. 4(c). Thus, we have

$$\overline{\mathbf{B}}_i^{(pt)} = \begin{bmatrix} \mathbf{B}_{lp,i}^{(pt)} \\ \hdashline \mathbf{B}_{gp,i}^{(pt)} \end{bmatrix} = \begin{bmatrix} \overline{\mathbf{B}}_{low}^{(pt)} & \overline{\mathbf{B}}_{up}^{(pt)} & \cdots & \overline{\mathbf{B}}_{low}^{(pt)} & \overline{\mathbf{B}}_{up}^{(pt)} \\ \hdashline \overline{\mathbf{B}}_{gp}^{(pt)} & \overline{\mathbf{B}}_{gp}^{(pt)} & \cdots & \overline{\mathbf{B}}_{gp}^{(pt)} & \overline{\mathbf{B}}_{gp}^{(pt)} \end{bmatrix}_{(f+s) \times 2lf},$$

where $\overline{\mathbf{B}}_{low}^{(pt)}$ and $\overline{\mathbf{B}}_{up}^{(pt)}$ are lower and upper triangular matrices of size $f \times f$, respectively, and $\overline{\mathbf{B}}_{gp}^{(pt)}$ is an all-one matrix of size $s \times f$, s represents the number of global CNs. For $f = 2$, $l = 2$ and $s = 1$, we have

$$\overline{\mathbf{B}}_i^{(pt)} = \left[\begin{array}{cccccccc} 1 & 0 & 1 & 1 & 1 & 0 & 1 & 1 \\ 1 & 1 & 0 & 1 & 1 & 1 & 0 & 1 \\ \hdashline 1 & 1 & 1 & 1 & 1 & 1 & 1 & 1 \end{array}\right], \quad 0 \le i \le t-1,$$

refer to Fig. 4(c).

Fig. 4(d) depicts the protograph of the GC-LDPC ensemble which is formed by applying the global edge spreading operation of $\overline{\mathbf{B}}_i^{(pt)}$. We call this GC-LDPC ensemble the *type-2 GC-LDPC ensemble*. The protomatrix corresponding to such protograph of Fig. 4(d) is

$$\overline{\mathbf{B}}_{gc,1}^{(pt)} = \left[\begin{array}{cccc} \mathbf{B}_{lp,0}^{(pt)} & & & \\ & \mathbf{B}_{lp,1}^{(pt)} & & \\ & & \ddots & \\ & & & \mathbf{B}_{lp,t-1}^{(pt)} \\ \hdashline \mathbf{B}_{gp,0}^{(pt)} & \mathbf{B}_{gp,1}^{(pt)} & \cdots & \mathbf{B}_{gp,t-1}^{(pt)} \end{array}\right]_{(ft+s)\times 2lft}.$$

In order to get a better view of this GC-LDPC ensemble, we perform the inter-column permuting on $\overline{\mathbf{B}}_{gc,1}^{(pt)}$ based on the pattern $< p_{c,i} >$ in (5), where $p_{c,i}$ is the original column position of the ith permuted column.

$$< p_{c,i} > = \left\langle i_1 + 2lfi_2 + i_3 + 2fti_4 \right\rangle, \tag{5}$$

where $0 \le i = (i_1 + i_2 f + i_3 ft + 2i_4 ft) \le 2lft - 1$, $0 \le i_1 \le f-1$, $0 \le i_2 \le t-1$, $0 \le i_3 \le 1$, and $0 \le i_4 \le l-1$. After the inter-column permuting, the protomatrix of the type-2 GC-LDPC ensemble is

$$\mathbf{B}_{gc,2}^{(pt)} = \left[\begin{array}{ccccc} \overline{\mathbf{B}}_{low}^{(pt)} & & \overline{\mathbf{B}}_{up}^{(pt)} & & \\ & \ddots & & \ddots & \cdots \\ & \overline{\mathbf{B}}_{low}^{(pt)} & & \overline{\mathbf{B}}_{up}^{(pt)} & \\ \hdashline \overline{\mathbf{B}}_{gp}^{(pt)} & \cdots & & \cdots & \cdots \end{array}\right]_{(ft+s)\times 2lft}.$$

The design rate of a type-2 protograph-based GC-LDPC ensemble with n_{tr} transmitted VNs in the protograph is

$$R_d = \frac{2lft - (ft+s)}{n_{tr}}.$$

Note that, in the case of $n_{tr} = n_v = 2lft$ (there is no puncture) the design rate is $R_d = 1 - \frac{1}{2l} - \frac{s}{2lft}$. Since $f = 2$, $l = 2$, $s = 1$, and $t = 2$, the design rate of the type-2 protograph-based GC-LDPC ensemble shown in Fig. 4 is $R_d = 1 - 1/4 - 1/16 = 0.6875$.

It is easy to see that replacing the nonzero elements in the protomatrices of the type-1/type-2 protograph-based GC-LDPC ensembles by circulants gives rise to the cascaded/interleaved type of GC-LDPC codes [21]. For this reason, we can design GC-QC-LDPC codes by analyzing the decoding thresholds for protograph-based GC-LDPC ensembles, which are presented in the subsequent sections.

IV. ITERATIVE DECODING CONVERGENCE ANALYSIS OVER BUECS-G

In this section, we introduce the GA and discuss the P-EXIT analysis over BuECs-G.

A. GAUSSIAN APPROXIMATION OF LDPC CODES OVER BUECS-G

Let $\left(\lambda(x) = \sum_{i=2}^{d_l} \lambda_i x^{i-1}, \rho(x) = \sum_{i=2}^{d_r} \rho_i x^{i-1}\right)$ be the "edge-perspective" degree-distribution pair, where λ_i (ρ_i) is the fraction of edges in the Tanner graph connected to degree-i VNs (CNs) and d_l (d_r) is the maximum degree of VNs (CNs). Let

$$\Lambda_i = \frac{\lambda_j/j}{\sum_{i=2}^{d_l} \lambda_i/i}$$

be the fraction of VNs that have degree i.

Let $L_i = \log[p(y_i|x_i = 1)/p(y_i|x_i = -1)]$ be the channel LLRs of code bit x_i for $0 \le i \le N-1$ (without loss of generality, we will drop the index i). For the BuEC-G, the probability density function (pdf) of the LLR from the channel can be written as

$$f_{mix}(L) = \frac{1 - \varepsilon_{VN}^{(0)}}{\sqrt{4\pi m_{ch}}} e^{-\frac{(L \pm m_{ch})^2}{4m_{ch}}} + \varepsilon_{VN}^{(0)} \delta(L), \tag{6}$$

where $m_{ch} = \mathbb{E}[L|L \neq 0]$, $\varepsilon_{VN}^{(0)} = \varepsilon_{ch}$, and $\delta(\cdot)$ is a shifted delta function [4].

If at least one of the VNs connected to a CN is erased, this CN has zero LLR as its message [4]. Let $\varepsilon_{CN}^{(k)}$ be the probability that a CN message is equal to zero (representing the CN is "erased") at the kth iteration. We have

$$\begin{aligned} \varepsilon_{CN}^{(k)} &= \sum_{s=2}^{d_r} \Pr\{d_c = s\} \Pr\{u^{(k)} | d_c = s\} \\ &= \sum_{s=2}^{d_r} \rho_s (1 - \prod_{i=1}^{s-1} \Pr\{v_{i=1}^{(k)} \neq 0\}) \\ &= \sum_{s=2}^{d_r} \rho_s (1 - (1 - \varepsilon_{VN}^{(k)})^{s-1}) \\ &= 1 - \rho(1 - \varepsilon_{VN}^{(k)})^{s-1}, \end{aligned} \tag{7}$$

where the term $u_i^{(k)}$ ($v_i^{(k)}$) is the message of a CN (VN) emitting through the ith edge at the kth iteration (without loss of generality, we will drop the index i).

Similarly, if a VN is erased and all incident check messages are zeros, the VN takes zero LLR as its message. Let $\varepsilon_{VN}^{(k)}$ be the probability that a VN message is equal to zero (representing the VN is "erased") at the kth iteration. We have

$$\begin{aligned} \varepsilon_{VN}^{(k)} &= \Pr\{v^{(k)} = 0\} \\ &= \sum_{j=2}^{d_l} \Pr\{d_v = j\} \varepsilon_{VN}^{(0)} (\varepsilon_{CN}^{(k-1)})^{j-1} \\ &= \varepsilon_{VN}^{(0)} \sum_{j=2}^{d_l} \lambda_j (\varepsilon_{CN}^{(k-1)})^{j-1} \\ &= \varepsilon_{VN}^{(0)} \lambda(1 - \rho(1 - \varepsilon_{CN}^{(k-1)})). \end{aligned} \tag{8}$$

Let $m_{CN}^{(k)}$ be the mean value of the outgoing message from a CN at the kth iteration. The pdf of a variable message at the kth iteration can be factorized into three terms in (9), as shown at the bottom of this page.

Define

$$\phi(x) = \begin{cases} 1 - \frac{1}{\sqrt{4\pi x}} \int_{\mathbb{R}} \tanh \frac{u}{2} e^{-\frac{-(u-x)^2}{4x}} du, & \text{if } x > 0, \\ 1, & \text{if } x = 0. \end{cases}$$

Let $\mathcal{B}(m, n, \varepsilon_{CN}^{(k)})$ be the probability mass function of binomial distribution as follows

$$\mathcal{B}(m, n, \varepsilon_{CN}^{(k)}) = \binom{n}{m} (\varepsilon_{CN}^{(k)})^{(n-m)} (1 - \varepsilon_{CN}^{(k)})^m,$$

and $\binom{n}{m}$ is the binomial coefficient. The updated mean of the outgoing message from a CN can be given in (10), as shown at the bottom of this page. Let $Q(\cdot)$ be the Q-function of the standard normal distribution [4]. The bit-error probability at the kth iteration is given in (11), as shown at the bottom of this page.

For general binary-input memoryless output-symmetric channels, the general stability condition plays an important role in analyzing the upper bound on the threshold [41], and the stability condition is given in (12), as shown at the bottom of the next page. Based on this condition, we demonstrate some conclusions about the upper bound on thresholds in the following.

Theorem 2: For $\lambda'(0)\rho'(1) > 1$ and a given ε_{ch}, we have

$$\sigma_{mix}^2(\lambda, \rho) \le \left[2 \ln \left(\frac{\lambda'(0)\rho'(1)(1 - \varepsilon_{ch})}{1 - \lambda'(0)\rho'(1)\varepsilon_{ch}} \right) \right]^{-1} = \widetilde{\sigma}_{mix}^2,$$

where $\widetilde{\sigma}_{mix}^2$ is the upper bound on the threshold of σ_n^2 over the BuEC-G. Since,

$$\ln \frac{1 - \varepsilon_{ch}}{1 - \lambda'(0)\rho'(1)\varepsilon_{ch}} \ge 0,$$

we have

$$\begin{aligned} \widetilde{\sigma}_{mix}^2 &= \left[2 \ln \left(\lambda'(0)\rho'(1) \right) + 2 \ln \left(\frac{1 - \varepsilon_{ch}}{1 - \lambda'(0)\rho'(1)\varepsilon_{ch}} \right) \right]^{-1} \\ &\le \frac{1}{2 \ln \lambda'(0)\rho'(1)}, \end{aligned}$$

where the equality holds only for $\varepsilon_{ch} = 0$.

Theorem 3: For $\lambda'(0)\rho'(1) > 1$ and a given σ_n^2, we have

$$\varepsilon_{ch,mix}(\lambda, \rho) \le \frac{1 - \lambda'(0)\rho'(1)e^{-\frac{1}{2\sigma_n^2}}}{\lambda'(0)\rho'(1)(1 - e^{-\frac{1}{2\sigma_n^2}})} = \widetilde{\varepsilon}_{ch,mix},$$

where $\widetilde{\varepsilon}_{ch,mix}$ is the upper bound on the threshold of ε_{ch} over the BuEC-G. We have

$$\begin{aligned} \widetilde{\varepsilon}_{ch,mix} &= \frac{1}{\lambda'(0)\rho'(1)} + \frac{1 - \lambda'(0)\rho'(1)}{\lambda'(0)\rho'(1)(1 - e^{-\frac{1}{2\sigma_n^2}})} e^{-\frac{1}{2\sigma_n^2}} \\ &\le \frac{1}{\lambda'(0)\rho'(1)}, \end{aligned}$$

where the equality holds only for $\sigma_n^2 = 0$.

B. PROTOGRAPH-BASED EXIT ANALYSIS OF LDPC CODES OVER BUECS-G

The P-EXIT technique is a precise and effective tool for estimating the decoding thresholds of protograph-based LDPC code ensembles, and applicable for both the AWGN channel

$$\begin{aligned} f_{mix}^{(k)}(L) &= \varepsilon_{VN}^{(k)} \delta(L) + (1 - \varepsilon_{VN}^{(k)}) h^{(k)}(L) = \varepsilon_{VN}^{(k)} \delta(L) + \varepsilon_{VN}^{(0)} \left\{ \sum_{j=2}^{d_l} \lambda_j \sum_{i=1}^{j-1} \mathcal{B}(i, j-1, \varepsilon_{CN}^{(k-1)}) \mathcal{N}(i m_{CN}^{(k-1)}, 2i m_{CN}^{(k-1)}) \right\} \\ &\quad + (1 - \varepsilon_{VN}^{(0)}) \left\{ \sum_{j=2}^{d_l} \lambda_j \sum_{i=0}^{j-1} \mathcal{B}(i, j-1, \varepsilon_{CN}^{(k-1)}) \mathcal{N}(i m_{CN}^{(k-1)} + m_{ch}, 2i m_{CN}^{(k-1)} + 2m_{ch}) \right\} \end{aligned} \tag{9}$$

$$\begin{aligned} m_{CN}^{(k)} &= \sum_{s=2}^{d_r} \rho_s m_{CN|d_c=s}^{(k)} = \sum_{s=2}^{d_r} \rho_s \phi^{-1} \Bigg(1 - \frac{1}{(1 - \varepsilon_{VN}^{(k)})^{s-1}} \Bigg[\varepsilon_{VN}^{(0)} \sum_{j=2}^{d_l} \lambda_j \sum_{i=0}^{j-1} \mathcal{B}(i, j-1, \varepsilon_{CN}^{(k-1)}) \left(1 - \phi(i m_{CN}^{(k-1)}) \right) \\ &\quad + (1 - \varepsilon_{VN}^{(0)}) \sum_{j=2}^{d_l} \lambda_j \sum_{i=0}^{j-1} \mathcal{B}(i, j-1, \varepsilon_{CN}^{(k-1)}) \left(1 - \phi(i m_{CN}^{(k-1)} + m_{ch}) \right) \Bigg]^{s-1} \Bigg) \end{aligned} \tag{10}$$

$$\begin{aligned} P_e^{(k)} &= \varepsilon_{VN}^{(0)} \sum_{s=2}^{d_l} \Lambda_s \sum_{i=0}^{s} \mathcal{B}(i, s, \varepsilon_{CN}^{(k)}) Q\left(\sqrt{i m_{CN}^{(k)}/2} \right) + (1 - \varepsilon_{VN}^{(0)}) \sum_{s=2}^{d_l} \Lambda_s \sum_{i=0}^{s} \mathcal{B}(i, s, \varepsilon_{CN}^{(k)}) Q\left(\sqrt{(i m_{CN}^{(k)} + m_{ch})/2} \right) \\ &= \frac{\varepsilon_{VN}^{(0)}}{2} \sum_{s=2}^{d_l} \left(\Lambda_s (\varepsilon_{CN}^{(k)})^s \right) + \varepsilon_{VN}^{(0)} \sum_{s=2}^{d_l} \Lambda_s \sum_{i=1}^{s} \mathcal{B}(i, s, \varepsilon_{CN}^{(k)}) Q\left(\sqrt{i m_{CN}^{(k)}/2} \right) \\ &\quad + (1 - \varepsilon_{VN}^{(0)}) \sum_{s=2}^{d_l} \Lambda_s \sum_{i=0}^{s} \mathcal{B}(i, s, \varepsilon_{CN}^{(k)}) Q\left(\sqrt{(i m_{CN}^{(k)} + m_{ch})/2} \right) \end{aligned} \tag{11}$$

and BEC [34]. In the following, we generalize the P-EXIT analysis to the BuEC-G.

For the VN of code bit x, let I_{EV} be the extrinsic mutual information (MI) between x and the outgoing message, and I_{AV} be the (*a priori*) MI between x and incoming message. $J(\sigma)$ represents the extrinsic MI of the binary-input AWGN channel and is given in [39]:

$$J(\sigma) = 1 - \int_{-\infty}^{+\infty} \mathcal{N}\Big(\frac{\sigma^2}{2}, \sigma^2\Big)(1 + e^{-x})dx. \tag{13}$$

We define a key parameter $J_{GB}(\sigma)$ for approximating the extrinsic MI of the BuEC-G as follows

$$J_{GB}(\sigma, \varepsilon_{ch}) = (1 - \varepsilon_{ch}) \sum_{j=2}^{d_l} \lambda_j J\Big(\sqrt{(j-1)\sigma^2 + \sigma_{ch}^2}\Big) + \varepsilon_{ch} \sum_{j=2}^{d_l} \lambda_j J\Big(\sqrt{(j-1)\sigma^2}\Big). \tag{14}$$

From (9), we adopt the consistent-Gaussian assumption [42] for the extrinsic-information input/output of VN processors. Let $p_L(L|x)$ be the pdf of the LLR for the variable message. Then, the extrinsic MI between x and the outgoing message is given in (15), as shown at the bottom of this page. In (15), equality (a) follows by the consistency condition, i.e., $p_L(L|x = -1) = p_L(-L|x = +1)$. Expressing I_{EV} as a function of I_{AV} yields

$$\begin{aligned} I_{EV} &= (1 - \varepsilon_{ch}) \sum_{j=2}^{d_l} \lambda_j \sum_{i=0}^{j-1} \mathcal{B}(i, j-1, \varepsilon_{CN}) J\Big(\sqrt{i\sigma^2 + \sigma_{ch}^2}\Big) \\ &\quad + \varepsilon_{ch} \sum_{j=2}^{d_l} \lambda_j \sum_{i=1}^{j-1} \mathcal{B}(i, j-1, \varepsilon_{CN}) J\Big(\sqrt{i\sigma^2}\Big) + \varepsilon_{VN}^{(k)} \\ &\approx J_{GB}(\sigma, \varepsilon_{ch}) \\ &= (1 - \varepsilon_{ch}) \sum_{j=2}^{d_l} \lambda_j J\Big(\sqrt{(j-1)[J^{-1}(I_{AV})]^2 + \sigma_{ch}^2}\Big) \\ &\quad + \varepsilon_{ch} \sum_{j=2}^{d_l} \lambda_j J\Big(\sqrt{(j-1)[J^{-1}(I_{AV})]^2}\Big). \end{aligned} \tag{16}$$

Let I_{EC} be the extrinsic MI between the code bit x and the message passing from the CN to x, and I_{AC} be the (*a prior*) MI between the code bit x and the corresponding incoming message of the CN. We have

$$I_{EC} = \sum_{j=2}^{d_r} \rho_j \theta(I_{AC}), \tag{17}$$

where $\theta(\cdot)$ denotes the MI function of the *a priori* information for the input of the CN processor. However, determining the mean and variance of the outgoing message from a CN processor is not straightforward [32], [33]. A simple approximation of the CN EXIT function is given by

$$\begin{aligned} I_{EC} &\approx 1 - \sum_{j=2}^{d_r} \rho_j I_{EV}(\sigma_{ch} = 0, I_{AV} \leftarrow 1 - I_{AC}) \\ &= 1 - \sum_{j=2}^{d_r} \rho_j \sum_{i=2}^{d_l} \lambda_i J\Big(\sqrt{(j-1)[J^{-1}(1 - I_{AC})]^2}\Big). \end{aligned} \tag{18}$$

In the following, we propose an improved P-EXIT technique for the BuEC-G. Considering protograph, let $I_{EV}^{(k)}(i,j)$ be the extrinsic MI between the outgoing message from the jth VN (v_j) to the ith CN (c_i) at the kth iteration and the code bit x_j (associated with v_j), where $0 \le i \le n_c$ and $0 \le j \le n_v$. Similarly, let $I_{EC}^{(k)}(i,j)$ be the extrinsic MI between the message outgoing message from c_i to v_j at the kth iteration and x_j, $I_{ch}(j)$ be the channel MI at the input of the jth VN (v_j), and $I_{\mathrm{CMI}}^{(k)}(j)$ be the cumulative MI of v_j at the kth iteration.

Let $\varepsilon_{ch,j}$ be the erasure probability of v_j over the BuEC-G for $0 \le j \le n_v$, and

$$\delta_{ij} = \begin{cases} 1, & \text{if } i = j, \\ 0, & \text{otherwise.} \end{cases}$$

Since, $I_{EC}^{(k-1)}(i,j)$ $\big(I_{EV}^{(k)}(i,j)\big)$ acts as *a priori* MI in calculation of $I_{EV}^{(k)}(i,j)$ $\big(I_{EC}^{(k-1)}(i,j)\big)$, following (16) and (18), $I_{EV}^{(k)}(i,j)$, $I_{CMI}^{(k)}(j)$, and $I_{EC}^{(k)}(i,j)$ can be computed in (19), (20), and (21), as shown at the bottom of the next page, respectively.

$$\lambda'(0)\rho'(1) < \Big(\int_{\mathbb{R}} f(x)e^{-x/2}dx\Big)^{-1} = \Big(\int_{\mathbb{R}} \Big[\varepsilon_{ch}\delta(x) + (1-\varepsilon_{ch})\sqrt{\frac{\sigma_n^2}{8\pi}} e^{\Big(-\frac{\big(x - \frac{2}{\sigma_n^2}\big)\sigma_n^2}{8}\Big)}\Big] e^{-x/2}dx\Big)^{-1} = \Big(\varepsilon_{ch} + (1-\varepsilon_{ch})e^{-\frac{1}{2\sigma^2}}\Big)^{-1} \tag{12}$$

$$\begin{aligned} I_{EV}(\sigma) &= 1 - \int_{-\infty}^{+\infty} p_L(L|x=+1)\log_2\Big(1 + \frac{p_L(L|x=-1)}{p_L(L|x=+1)}\Big)dL \overset{(a)}{=} 1 - \int_{-\infty}^{+\infty} f_{mix}^{(k)}(L)\log_2(1 + e^{-L})dL \\ &= 1 - \varepsilon_{VN}^{(k)} - \varepsilon_{ch} \int_{-\infty}^{+\infty} \sum_{j=2}^{d_l} \lambda_j \sum_{i=1}^{j-1} \mathcal{B}(i, j-1, \varepsilon_{CN}) \mathcal{N}\Big(i\frac{\sigma^2}{2}, i\sigma^2\Big)\log_2(1 + e^{-L})dL \\ &\quad - (1 - \varepsilon_{ch}) \int_{-\infty}^{+\infty} \sum_{j=2}^{d_l} \lambda_j \sum_{i=0}^{j-1} \mathcal{B}(i, j-1, \varepsilon_{CN}) \mathcal{N}\Big(i\frac{\sigma^2}{2} + \frac{\sigma_{ch}^2}{2}, i\sigma^2 + \sigma_{ch}^2\Big)\log_2(1 + e^{-L})dL \end{aligned} \tag{15}$$

V. DESIGN OF GC-LDPC CODES FOR BUECS-G

We now present an edge spreading optimization method for minimizing the gap between the capacity and the iterative decoding threshold of GC-LDPC codes over BuECs-G. The proposed method is based on predicting the iterative decoding threshold of GC-QC-LDPC codes as mentioned in Section III within a given range of code rates and code lengths.

For GC-QC-LDPC codes, suppose that the range of code rate R, the range of the code length N, and the field GF(q) are given. Denote R_{max} (R_{min}), N_{max} (N_{min}), and $W_{\text{GA/P-EXIT}}$ as the maximum (minimum) value of R, the maximum (minimum) value of N, and the weighted mean value of the gap between the capacity and the iterative decoding threshold for GC-LDPC codes over BuECs-G with different parameters based on GA/P-EXIT, respectively. The optimization of the edge spreading for minimizing $W_{\text{GA/P-EXIT}}$ of GC-LDPC codes over BuECs-G can be divided into the following steps:

1) **Initialization.** Set the initial metric $W_{\text{GA/P-EXIT}} \gg 0$.
2) **Global Edge Spreading Operation.** By applying the *global edge spreading* operation mentioned in Section III, we form the protograph-based GC-LDPC codes with all sets of parameters for given R_{max} (R_{min}), N_{max} (N_{min}), and q. Enumerate all sets of parameters for GC-QC-LDPC codes. For type-1 GC-QC-LDPC codes, the parameters (m, n, t, s) satisfy:

$$\begin{cases} t \in \{2, 3, \dots, q-1\}, \\ n \in \{2, 3, \dots, (q-1)/t\}, \\ m \in \{1, 2, \dots, n\}, \\ s \in \{1, 2, \dots, q - mt - 1\}, \\ nt(q-1) \in \{N_{min}, N_{min}+1, \dots, N_{max}\}, \\ R_{min} \le 1 - m/n - s/nt \le R_{max}, \end{cases} \tag{22}$$

where p is a prime factor of q satisfying $q^d - 1 = pa$ with $d, a \in \mathbb{N}$. For type-2 GC-QC-LDPC codes, the parameters (l, f, t, s) satisfy:

$$\begin{cases} t \in \{2, 3, 4\}, \\ f \in \{2, 3, \dots, \frac{p}{4t}\}, \\ l \in \{2, 3, \dots, \frac{p}{2tf}\}, \\ s \in \{1, 2, \dots, p - tf\}, \\ 2ltfp \in \{N_{min}, N_{min}+1, \dots, N_{max}\}, \\ R_{min} \le 1 - 1/2l - s/2lft \le R_{max}. \end{cases} \tag{23}$$

Notice that these optimized parameters are obtained by the construction methods mentioned in Section III. The code length N and the design rate R_d of type-1 GC-QC-LDPC codes are equal to $nt(q-1)$ and $1 - m/n - s/t$, respectively. Since the base matrix of such GC-LDPC code is formed over GF(q), we have $2 \le t \le q$, $nt \le q-1$, $1 \le m \le n$, and $1 \le s \le q - 1 - mt$. Similarly, the code length N and the design rate R_d of type-2 GC-QC-LDPC codes are equal to $2ltfp$ and $1 - 1/2l - s/2lft$, respectively. Here, the parameters of type-2 GC-QC-LDPC codes satisfy $2 \le t \le 4$, $l \ge 2$, $2ltf \le p$, and $1 \le s \le p - tf$.
3) **Compute Metric.** Compute the metric $W_{\text{GA/P-EXIT}}$ as follows:

$$\min_{\arg\{\mathbf{B}^{(pt)}\}} W_{\text{GA/P-EXIT}} = \sum_{d=0}^{D-1} w_d \left\{ K_{\text{GA/P-EXIT}}\left(\mathbf{B}^{(pt)}, \varepsilon_{ch}\right) - K\left(\varepsilon_{ch}, R\right) \right\},$$
$$\text{s.t. } R_d = \begin{cases} 1 - m/n - s/nt, & \text{for type-1}, \\ 1 - 1/2l - s/2lft, , & \text{for type-2}, \end{cases} \tag{24}$$

where $\{w_d\}$ are positive real weighting factors, $K_{\text{GA/P-EXIT}}(\cdot)$ is the bit SNR threshold computed by GA/P-EXIT for the corresponding protomatrix $\mathbf{B}^{(pt)}$ of (m, n, t, s) or (l, f, t, s), $K(\cdot)$ is the bit SNR corresponding to the capacity of the BuEC-G for a coding rate of R.
4) **Termination.** Search for the optimal global edge spreading form (as mentioned earlier, the optimal global edge spreading forms are determined by the corresponding set of parameters $(m, n, t, s)/(l, f, t, s)$) which leads to minimize the $W_{\text{GA/P-EXIT}}$.

Next, we present two approaches to design the GC-QC-LDPC codes with a given range of code rates and code lengths for the GA and the P-EXIT, respectively.

A. CODE DESIGN BASED ON GAUSSIAN APPROXIMATION

The GA procedure for predicting the iterative decoding threshold $K_{GA}(\mathbf{B}^{(pt)}, \varepsilon_{ch})$ on the BuEC-G can be summarized as follows:

1) **Initialization.** Select the bit SNR associated to the channel input which is denoted by E_b/N_0. Set $\varepsilon_{VN}^{(0)} = \varepsilon_{ch}$, $\varepsilon_{CN}^{(0)} = 1 - \rho(1 - \varepsilon_{VN}^{(0)})$,

$$I_{EV}^{(k)}(i,j) = (1 - \varepsilon_{ch,j}) J\left(\sqrt{\sum_{d=1}^{M} (b_{dj}^{(pt)} - \delta_{id})[J^{-1}(I_{EC}^{(k-1)}(d,j))]^2 + I_{ch}^2(j)}\right) + \varepsilon_{ch,j} J\left(\sqrt{\sum_{d=1}^{M} (b_{dj}^{(pt)} - \delta_{id})[J^{-1}(I_{EC}^{(k-1)}(d,j))]^2}\right) \tag{19}$$

$$I_{CMI}^{(k)}(j) = (1 - \varepsilon_{ch,j}) J\left(\sqrt{\sum_{d=1}^{M} (b_{dj}^{(pt)})[J^{-1}(I_{EC}^{(k-1)}(d,j))]^2 + I_{ch}^2(j)}\right) + \varepsilon_{ch,j} J\left(\sqrt{\sum_{d=1}^{M} (b_{dj}^{(pt)})[J^{-1}(I_{EC}^{(k-1)}(d,j))]^2}\right) \tag{20}$$

$$I_{EC}^{(k)}(i,j) = 1 - J\left(\sqrt{\sum_{d=1}^{N} (b_{id}^{(pt)} - \delta_{dj})[J^{-1}(1 - I_{EV}^{(k-1)}(i,d))]^2}\right) \tag{21}$$

$$m_{ch} = 4(RE_b/N_0),$$
$$P_e^{(0)} = \varepsilon_{VN}^{(0)}/2 + (1-\varepsilon_{VN}^{(0)})Q(\sqrt{m_{ch}/2}),$$
$$m_{CN}^{(0)} = 0,\ k=0,\ T_{max} \gg 1,\ \text{ and } 0 < \xi_1 \ll 1,$$

where T_{max} is the maximum iteration number of decoder.

2) **Update operation.** $k = k+1$; Update $\varepsilon_{CN}^{(k)}$, $\varepsilon_{VN}^{(k)}$, $m_{CN}^{(k)}$, and $P_e^{(k)}$ based on (7), (8), (10), and (11), respectively;
3) **Stopping criterion.** If $P_e^{(k)} \le \xi_1$ or $k > T_{max}$, then stop; otherwise, go to step 2).

This algorithm converges only when E_b/N_0 is above the threshold which is the minimum value of E_b/N_0 for $P_e \le \xi_1$. We define the E_b/N_0 threshold computed with GA as

$$K_{GA} = \inf\left\{\frac{E_b}{N_0} \in \mathbb{R}\middle| P_e \le \xi_1,\ \text{for } k \to \infty \text{ and } 0 < \xi_1 \ll 1\right\}. \tag{25}$$

B. CODE DESIGN BASED ON P-EXIT

Based on the P-EXIT analysis defined in Section IV-B, we present an improved P-EXIT algorithm to calculate the decoding threshold for GC-QC-LDPC codes over the BuEC-G. The detailed P-EXIT algorithm is as follows:

1) **Initialization.** Select the bit SNR associated to the channel input of the jth VN which is denoted by $(E_b/N_0)_j$. Initialize a vector $\boldsymbol{\sigma}_{ch} = [\sigma_{ch}(0), \ldots, \sigma_{ch}(N-1)]$, where $\sigma_{ch,j}^2$ is the variance of the consistent-Gaussian input from the channel to the jth VN. Set $k = 1$, $I_{ch}(j) = J_{GB}(\sigma_{ch,j})$, $\forall j = 0, \ldots, N-1$, with

$$\sigma_{ch,j}^2 = 8R(E_b/N_0)_j,$$
$$(E_b/N_0)_j = \begin{cases} 0, & \text{if the } j\text{-th VN is punctured,} \\ E_b/N_0, & \text{otherwise.} \end{cases}$$

Set $T_{max} \gg 1$ and $\varepsilon_{ch,j} = F_j/F$, where F is the size of the CPM and F_j is the number of erasure bits in the jth CPM.

2) **VN to CN update.** For $j \in [0, N-1]$ and $i \in [0, M-1]$, update $I_{EV}^{(k)}(i,j)$ in (19).
3) **CN to VN update.** For $j \in [0, N-1]$ and $i \in [0, M-1]$, update $I_{EC}^{(k)}(i,j)$ in (21).
4) **Cumulative MI evaluation.** For $j \in [0, N-1]$, update $I_{\text{CMI}}^{(k)}(j)$ in (20).
5) **Stopping criterion.** If $k > T_{max}$ or $I_{\text{CMI}}^{(k)}(j) \le 1-\xi_2$ for all j, then stop; otherwise, $k = k+1$ and go to step 2).

This algorithm converges only when E_b/N_0 is above the threshold which is the minimum value of E_b/N_0 for all $I_{CMI}^{(k)}(j) \le 1-\xi_2$. Define the E_b/N_0 threshold computed with P-EXIT by

$$K_{\text{P-EXIT}} = \inf\left\{\frac{E_b}{N_0} \in \mathbb{R}\middle| I_{\text{CMI}}^{(k)}(j) \le 1-\xi_2, \textit{for } k \to \infty,\right.$$
$$\left. 0 < \xi_2 \ll 1 \text{ and } j \in [0, N-1]\right\}. \tag{26}$$

For the REC-G model, $\varepsilon_{ch,j}$ is equal to the random erasure probability. For the GEC-G model, we can obtain F_j by two methods. For the first method, $\varepsilon_{ch,j}$ is approximated by the average erasure probability over the GEC-G. Thus, $F_j = \varepsilon_{ch}F$ for all j. For the second method, F_j can be obtained via Monte Carlo simulations. Based on the Gilbert-Elliott erasures model, we generate many sequences of binary noise digits with the length FN. The value of F_j is approximated by the average number of the erasure bits in the jth F elements of these sequences.

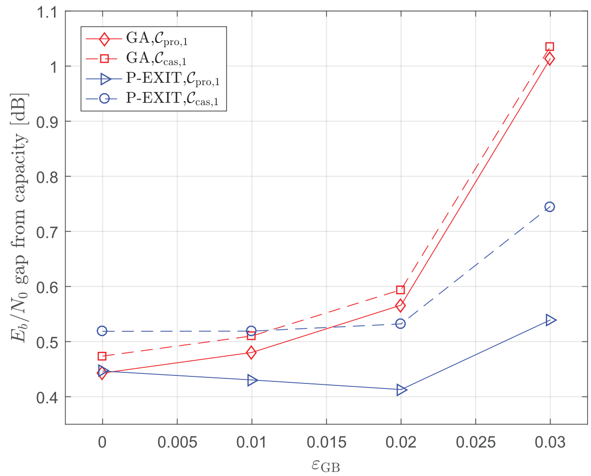

FIGURE 5. The gaps between the GA/P-EXIT thresholds and the capacity of the cascaded type of GC-QC-LDPC codes. ($R_d = 20/21$, $N = 15876$ bits, $\varepsilon_G = 0.0$, $\varepsilon_B = 0.5$, $\triangle_B = 10$, and $\varepsilon_{GB} = 0.00, 0.01, 0.02, 0.03$).

C. SIMULATION PERFORMANCE EVALUATION

In this subsection, we use several examples to illustrate the proposed methods for designing two types (i.e., cascaded and interleaved) of proposed GC-QC-LDPC codes. We will show that the proposed GC-QC-LDPC codes perform well for both the AWGN channel and the GEC-G.

Example 1: Consider a cascaded type of GC-QC-LDPC code which has a code rate of 20/21, code length of 15876 bits and the CPM size of 126. As shown in Fig. 5, we evaluate GA and P-EXIT thresholds between a well-designed cascaded type of GC-QC-LDPC code $\mathcal{C}_{cas,1}$ for the AWGN channel in [22] and a proposed type-1 protograph-based (cascaded type) GC-QC-LDPC code $\mathcal{C}_{pro,1}$ which is designed for the GEC-G by the mentioned above method. It is assumed that the erasure probabilities on the GEC-G in the "G" state and "B" state are $\varepsilon_G = 0.0$ and $\varepsilon_B = 0.5$, respectively, if not specified. The metric W_{GA} and W_{P-EXIT} in (24) are evaluated by the GA and P-EXIT at every erasure probability ε_{GB} between 0 and 0.03 with a 0.01 step and $\triangle_B = 10$, respectively. The size of base matrices and CPMs for $\mathcal{C}_{cas,1}$ and $\mathcal{C}_{pro,1}$ are 6×126 and 126×126, respectively. The sets of parameters (m, n, t, s) for $\mathcal{C}_{cas,1}$ and $\mathcal{C}_{pro,1}$ are (1, 42, 3, 3) and (2, 63, 2, 2), respectively. The GA/P-EXIT thresholds of $\mathcal{C}_{cas,1}$ and $\mathcal{C}_{pro,1}$ are shown in Table 1. We see that the designed QC-LDPC code $\mathcal{C}_{pro,1}$ shows better thresholds in both GA and P-EXIT. For $\mathcal{C}_{cas,1}$, the gaps between the P-EXIT thresholds and the capacity are less than the gaps between the GA thresholds and the capacity ($\varepsilon_{GB} > 0.02$).

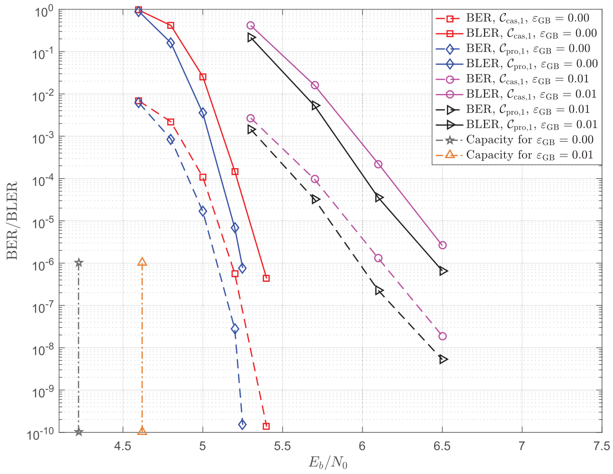

FIGURE 6. The BER/BLER performances of the cascaded type of GC-QC-LDPC codes over the GEC-G and BPSK signaling (MSA decoder, maximum iteration number= 50, rate= 20/21, code length= 15876 bits, $\varepsilon_G = 0.0$, $\varepsilon_B = 0.5$, $\Delta_B = 10$, and $\varepsilon_{GB} = 0.00, 0.01$).

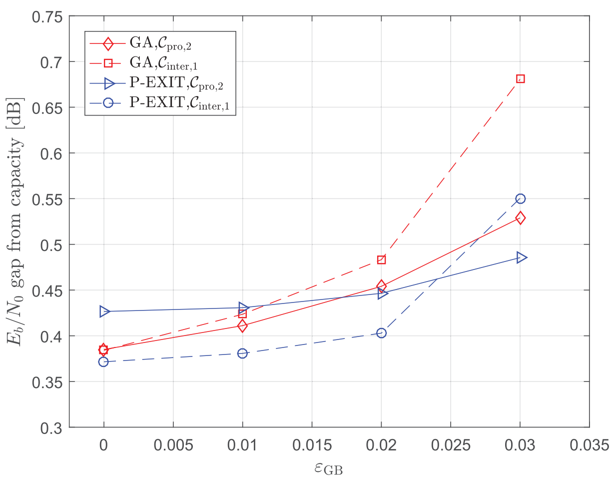

FIGURE 7. The gaps between the GA/P-EXIT thresholds and the capacity of the interleaved type of GC-QC-LDPC codes. ($R_d = 0.9$ and 0.8958, $N = 15240$ and 14976 bits, $\varepsilon_G = 0.0$, $\varepsilon_B = 0.5$, $\Delta_B = 10$, and $\varepsilon_{GB} = 0.00, 0.01, 0.02, 0.03$).

TABLE 1. The GA/P-EXIT Thresholds for the Cascaded Type of GC-QC-LDPC Codes over the GEC-G ($\varepsilon_G = 0.0$, $\varepsilon_B = 0.5$, $\Delta_B = 10$, $\xi_1 = 10^{-4}$, and $\xi_2 = 10^{-3}$).

Code	Method	ε_{GB}			
		0.00	0.01	0.02	0.03
$\mathcal{C}_{cas,1}$	GA	4.6856	5.1221	5.7061	6.7474
$\mathcal{C}_{pro,1}$		4.6548	5.0922	5.6781	6.7255
$\mathcal{C}_{cas,1}$	P-EXIT	4.7306	5.1310	5.6440	6.4572
$\mathcal{C}_{pro,1}$		4.6584	5.0423	5.5249	6.2513

Fig. 6 depicts the BER and BLER performance for $\mathcal{C}_{cas,1}$ and $\mathcal{C}_{pro,1}$ over the GEC-G with BPSK signaling. It is assumed that all the simulations are performed using the min-sum algorithm (MSA) [43] with the maximum iteration number 50, if not specified. The proposed GC-QC-LDPC code performs better than the existing well-designed GC-QC-LDPC code over the AWGN channel and GEC-G.

TABLE 2. The GA/P-EXIT Thresholds for the interleaved Type of GC-QC-LDPC Codes over the GEC-G ($\varepsilon_G = 0.0$, $\varepsilon_B = 0.5$, $\Delta_B = 10$, $\xi_1 = 10^{-4}$, and $\xi_2 = 10^{-3}$).

Code	Method	ε_{GB}			
		0.00	0.01	0.02	0.03
$\mathcal{C}_{inter,1}$	GA	3.6417	3.8812	4.1408	4.4382
$\mathcal{C}_{pro,2}$		3.5628	3.7888	4.0318	4.3066
$\mathcal{C}_{inter,1}$	P-EXIT	3.6292	3.8384	4.0605	4.3080
$\mathcal{C}_{pro,2}$		3.6043	3.8085	4.0242	4.2632

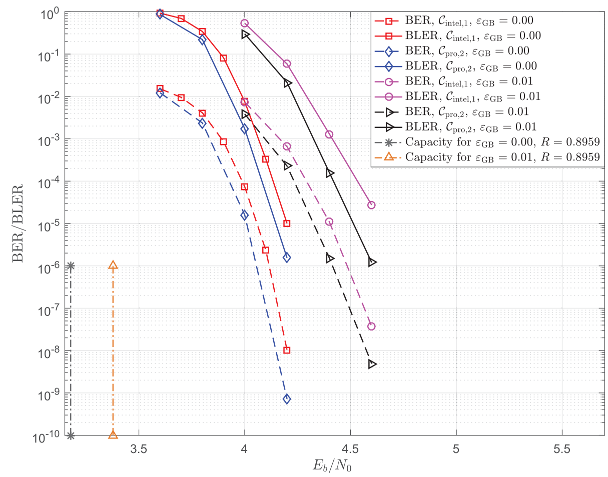

FIGURE 8. The BER/BLER performances of the interleaved type of GC-QC-LDPC codes over the GEC-G with BPSK signaling (MSA decoder, maximum iteration number= 50, rate= 0.9001 and 0.8959, code length= 15240 and 14976 bits, $\varepsilon_G = 0.0$, $\varepsilon_B = 0.5$, $\Delta_B = 10$, and $\varepsilon_{GB} = 0.00, 0.01$).

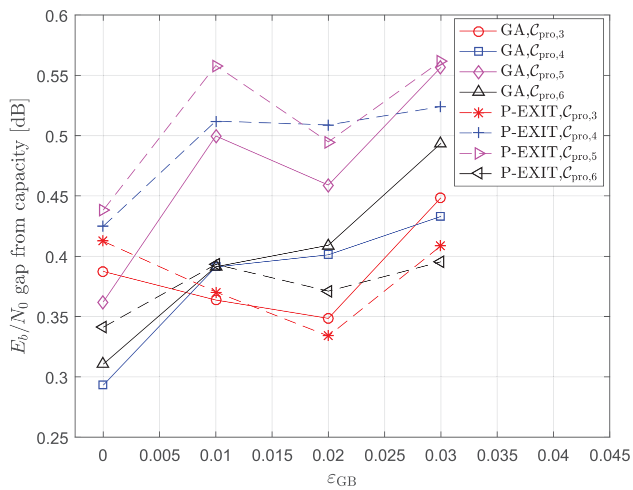

FIGURE 9. The gaps between the GA/P-EXIT thresholds and the capacity of $\mathcal{C}_{pro,\{3,4,5,6\}}$. ($\varepsilon_G = 0.0$, $\varepsilon_B = 0.5$, $\Delta_B = 10$, and $\varepsilon_{GB} = 0.00, 0.01, 0.02, 0.03$).

Example 2: We now consider the interleaved type of GC-QC-LDPC codes. After optimizing the GC-QC-LDPC code which has a code rate of 9/10 and code length of 15240 bits, we get the same set of parameters of the well-designed interleaved type of GC-QC-LDPC codes $\mathcal{C}_{inter,1}$ in [22]. Thus, we select another type-2 protograph-based (interleaved type) GC-QC-LDPC code $\mathcal{C}_{pro,2}$ which has

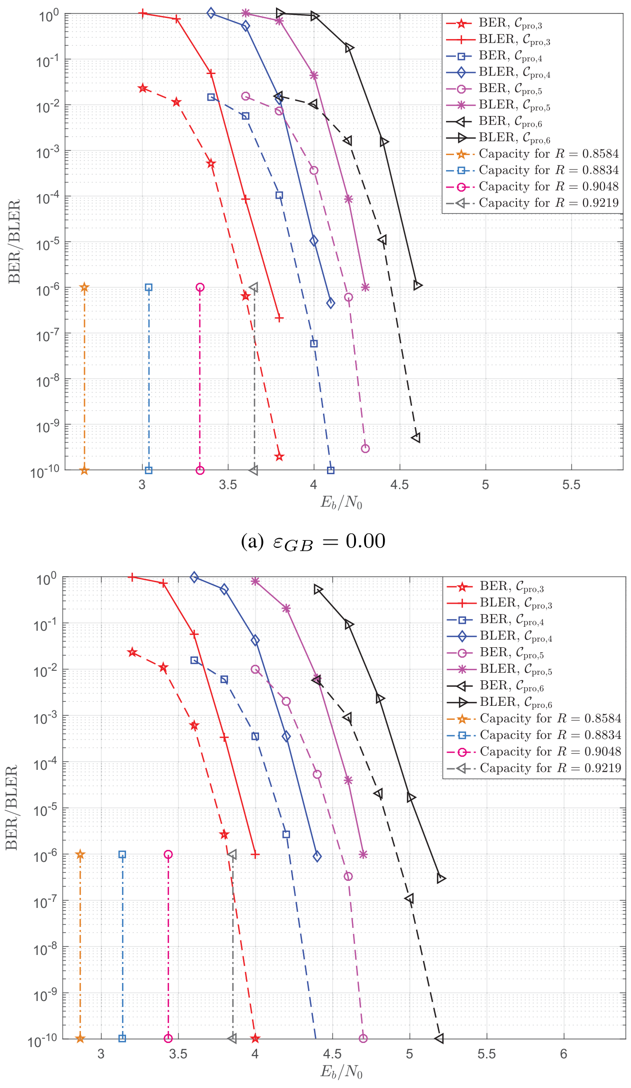

(a) $\varepsilon_{GB} = 0.00$

(b) $\varepsilon_{GB} = 0.01$ and $\triangle_B = 10$

FIGURE 10. The BER/BLER performances for $\mathcal{C}_{pro,\{3,4,5,6\}}$ over the GEC-G with BPSK signaling.

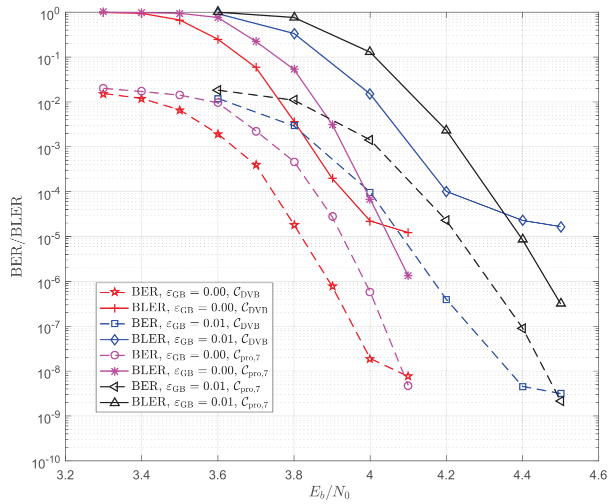

FIGURE 11. The BER/BLER performances of $\mathcal{C}_{pro,7}$ and $\mathcal{C}_{DVB}$ over the GEC-G with BPSK signaling (MSA decoder, maximum iteration number= 50, rate= 0.88895 and 0.88889, code length= 16272 and 16200 bits, $\varepsilon_G = 0.0$, $\varepsilon_B = 0.5$, $\Delta_B = 10$, and $\varepsilon_{GB} = 0.00, 0.01$).

TABLE 3. The Parameters for $\mathcal{C}_{pro,\{3,4,5,6\}}$.

Code	(l,f,t,s)	Field	CPM	Base Matrix	Code Length	Info. Length	Design Rate
$\mathcal{C}_{pro,3}$	(4,5,3,2)	157	156	17×120	18720	16069	0.8583
$\mathcal{C}_{pro,4}$	(5,4,3,2)	151	150	14×120	18000	15901	0.8833
$\mathcal{C}_{pro,5}$	(7,3,2,2)	211	210	8×84	17640	15961	0.9048
$\mathcal{C}_{pro,6}$	(8,4,2,2)	137	136	10×128	17408	16049	0.9219

coding rate of around 9/10 (i.e., 0.8959) and coding length of nearly 15240 (i.e., 14976) bits for further comparison. As shown in Fig. 7, we evaluate the GA and P-EXIT thresholds between $\mathcal{C}_{inter,1}$ and $\mathcal{C}_{pro,2}$. The metric $W_{P\text{-}EXIT}$ and W_{GA} in (24) are evaluated by the GA and P-EXIT at every erasure probability ε_{GB} between 0 and 0.03 with a 0.01 step and $\triangle_B = 10$, respectively. The size of the base matrices for $\mathcal{C}_{inter,1}$ and $\mathcal{C}_{pro,2}$ are 12×120 and 10×96, respectively. The size of CPMs for $\mathcal{C}_{inter,1}$ and $\mathcal{C}_{pro,2}$ are 127×127 and 156×156, respectively. The sets of parameters (l, f, t, s) for $\mathcal{C}_{inter,1}$ and $\mathcal{C}_{pro,2}$ are (6, 5, 2, 2) and (6, 4, 2, 2), respectively. Note that the design rates of $\mathcal{C}_{inter,1}$ and $\mathcal{C}_{pro,2}$ are 0.9 and 0.8958 respectively, which are slightly lower than the actual code rate (0.9001 and 0.8959). The GA/P-EXIT thresholds of $\mathcal{C}_{inter,1}$ and $\mathcal{C}_{pro,2}$ are shown in Table 2. Since the code rate of $\mathcal{C}_{pro,2}$ is slightly lower than that of $\mathcal{C}_{inter,1}$, $\mathcal{C}_{pro,2}$ shows better thresholds in both GA and P-EXIT.

Fig. 8 depicts the BER and BLER performances for $\mathcal{C}_{inter,1}$ and $\mathcal{C}_{pro,2}$ over the GEC-G with BPSK signaling. The proposed GC-QC-LDPC code performs well over the AWGN channel and GEC-G. At a BER of 10^{-7}, $\mathcal{C}_{inter,1}$ and $\mathcal{C}_{pro,2}$ perform 1.0 dB away from their corresponding capacity limits over the GEC-G.

Example 3: The proposed methods can also be used to construct GC-QC-LDPC codes with different rates. Here, we form four type-2 protograph-based (interleaved type) GC-QC-LDPC codes $\mathcal{C}_{pro,\{3,4,5,6\}}$ which have code rates of around 6/7, 8/9, 10/11, 12/13, and information lengths of nearly 16000 bits (see details in Table 3). We provide the GA and P-EXIT thresholds evaluations for $\mathcal{C}_{pro,\{3,4,5,6\}}$, as illustrated in Fig. 9. More specifically, for $\mathcal{C}_{pro,3}$, we find the thresholds from GA and P-EXIT are less than 0.45 dB away from the capacity over the GEC-G for $0.0 \leq \varepsilon_{GB} \leq 0.03$. Fig. 10 depicts the BER and BLER performances for $\mathcal{C}_{pro,\{3,4,5,6\}}$ over the GEC-G with BPSK signaling. We see that the proposed GC-QC-LDPC codes have no visible error-floor all the way down to the BER of 10^{-7} and perform with 1.2 dB away from their corresponding capacity limits over GECs-G.

Example 4: In order to compare the error performance of the proposed GC-QC-LDPC code, the well-designed LDPC code considered in the 2nd generation (2G) digital video broadcasting satellite (DVB-S2) standard [45] is adopted in this example, denoted by $\mathcal{C}_{DVB}$. The code rate and the code length of $\mathcal{C}_{DVB}$ are 8/9 and 16200 bits, respectively. Here, we form a type-2 protograph-based GC-QC-LDPC code $\mathcal{C}_{pro,7}$ which has a code rate of 0.88895, code length of 16272 bits and the CPM size of 226. The base matrix of $\mathcal{C}_{pro,7}$ is an 8×72 matrix over GF(227). The set of parameter (l, f, t, s) for $\mathcal{C}_{pro,7}$ is (6, 3, 2, 2). Fig. 11 gives BER/BLER performances of $\mathcal{C}_{pro,7}$ and $\mathcal{C}_{DVB}$ over the GEC-G with BPSK signaling. We see that the advantage of the proposed GC-QC-LDPC code is illustrated at the error-floor region.

VI. CONCLUSION

In this paper, we presented a new edge spreading operation to form the protograph-based GC-LDPC code, called the *global edge spreading*. We then proposed two types of protograph-based GC-LDPC codes. The first one was obtained by applying the *global edge spreading* operation to link the sequence of disjoint block LDPC codes together. The second one was formed by exploiting the *global edge spreading* and interleaved operations (inter-column permutation for the protomatrices) to some irregular (block) protograph-based LDPC codes. Moreover, we generalized the GA and P-EXIT analysis to the BuEC-G and gave the discussion on the stability condition. Based on the GA and the P-EXIT analysis, we presented two approaches to design the GC-QC-LDPC codes with given range of code rates and code lengths. Finally, we compared the decoding performances of proposed GC-LDPC codes with the existing well-designed GC-LDPC codes over the GEC-G. Numerical results have shown that the proposed GC-LDPC codes have better thresholds and performances than the existing well-designed GC-LDPC codes with similar parameters (code rates and code lengths), and the codes constructed by the proposed methods are effective against the erasures clustered in bursts with different rates. It should be noted that in some scenarios the decoder is difficult to accurately detect the duration and the occurrence locations of burst-noise, and we can also designate the burst-noise as the Gaussian noise with large variance (such as deep fading for wireless systems) or some specific impulsive noise (such as non-Gaussian pulses). These two cases were not discussed in this paper. Thus, future work includes applying the GA and the P-EXIT tools to design optimal protograph-based GC-LDPC codes with near-capacity thresholds over different types of channels.

ACKNOWLEDGMENT

The authors would like to thank Dr. Hengzhou Xu for his insightful discussions about the construction of discussions on the construction of GC-LDPC codes. They would also like to thank Miss Xin Dou for her valuable comments.

APPENDIX

SKETCH OF THE PROOF OF THEOREM 1

A sketch of the proof proceeds as follows. We here write X_i, Y_i, $\tilde{Y}_i$ and Z_i for the r.v. corresponding to the realizations of the symbols x_i, y_i, $\tilde{y}_i$, and z_i, respectively, where $i \in \{0, 1, \ldots, N-1\}$. Let X^N, Y^N, $\tilde{Y}^N$, and Z^N denote the N-fold sequences of X_i, Y_i, $\tilde{Y}_i$, and Z_i, respectively, where $X^N = [X_0, X_1, \ldots, X_{N-1}]$, $Y^N = [Y_0, Y_1, \ldots, Y_{N-1}]$, $\tilde{Y}^N = [\tilde{Y}_0, \tilde{Y}_1, \ldots, \tilde{Y}_{N-1}]$, and $Z^n = [Z_0, Z_1, \ldots, Z_{N-1}]$. First we will show that $\frac{1}{N} I(X^N, Y^N, Z^N) \leq (1 - \varepsilon_{ch}) C_{AWGN}$. Since X^N and Z^N are independent, we have

$$\begin{aligned} I(X^N, Y^N, Z^N) &= H(Y^N, Z^N) - H(Y^N, Z^N | X^N) \\ &= H(Y^N | Z^N) - H(Y^n | X^N, Z^N). \end{aligned} \tag{27}$$

For the first term in (27), we have

$$\begin{aligned} H(Y^N | Z^N) &\leq \sum_{i=0}^{N-1} H(Y_i | Z^N) \\ &\overset{(a)}{=} \sum_{i=0}^{N-1} H(Y_i | Z_i) \\ &= \sum_{i=0}^{N-1} \sum_{j=0}^{1} \Pr(Z_i = j) \cdot H(Y_i | Z_i = j) \\ &\overset{(b)}{=} \sum_{i=0}^{N-1} \Pr(Z_i = 0) \cdot H(\tilde{Y}_i), \end{aligned} \tag{28}$$

where equality (a) follows from the fact that Y_i is only related to Z_i in Z^n; equality (b) uses

$$H(Y_i | Z_i) = \begin{cases} 0, & Z_i = 1, \\ H(\tilde{Y}_i), & Z_i = 0. \end{cases}$$

The second term in (27) can be expanded as follows:

$$\begin{aligned} H(Y^N | X^N, Z^N) &= \sum_{i=0}^{N-1} H(Y_i | X^N, Z^N, Y^{i-1}), \\ &= \sum_{i=0}^{N-1} H(Y_i | X^N, Z_i, Y^{i-1}). \end{aligned} \tag{29}$$

Notice $\Pr(Z_i, Y_{i-1} = \tilde{Y}_{i-1}) = \Pr(Z_i, Z_{i-1} = 0)$ and $\Pr(Z_i, Y_{i-1} \neq \tilde{Y}_{i-1}) = \Pr(Z_i, Z_{i-1} = 1)$. We further manipulate (29) as

$$\begin{aligned} H(Y^N | X^N, Z^N) &= \sum_{i=0}^{N-1} H(Y_i | X^N, Z_i, Y^{i-1}) \\ &= \sum_{i=0}^{N-1} \sum_{j=0}^{1} \sum_{k=0}^{1} \Pr(Z_i = k, Z^{i-1} = j) \\ &\quad \times H(Y_i | X^N, Z_i = k, Z^{i-1} = j) \\ &\overset{(c)}{=} \sum_{i=0}^{N-1} \Pr(Z_i = 0) \cdot H(\tilde{Y}_i | X_i), \end{aligned} \tag{30}$$

where equality (c) uses

$$H(Y_i | X^N, Z_i) = \begin{cases} 0, & Z_i = 1, \\ H(\tilde{Y}_i | X_i), & Z_i = 0. \end{cases}$$

Combine equations (27), (28), and (30) to get

$$\begin{aligned}\frac{1}{N}I(X^N, Y^N, Z^N) &\leq \frac{1}{N}\sum_{i=0}^{N-1}\Pr(Z_i = 0)\cdot I(X_i; \tilde{Y}_i)\\ &\leq \frac{1}{N}\max_{p(x^N)}\sum_{i=0}^{N-1}\Pr(Z_i = 0)\cdot I(X_i; \tilde{Y}_i)\\ &= \frac{1}{N}\sum_{i=0}^{N-1}\Pr(Z_i = 0)\cdot\left[\max_{p(x^n)} I(X_i; \tilde{Y}_i)\right]\\ &= \frac{1}{N}\sum_{i=0}^{N-1}\Pr(Z_i = 0)\cdot C_{AWGN}\\ &\overset{(d)}{=} (1-\varepsilon_{ch})\cdot C_{AWGN}, \end{aligned} \tag{31}$$

where equality (d) follows from (2).

So, we only need to prove that there exists a distribution for which $\frac{1}{N}I(X^N, Y^N, Z^N)$ meets (31) with equality. Since it is similar to the proof of the capacity of a memoryless channel with burst erasure mentioned in [5], we omit it here for the sake of simplicity.

REFERENCES

[1] G. Forney, Jr., "Burst-correcting codes for the classic bursty channel," *IEEE Trans. Commun. Technol.*, vol. COM-19, no. 5, pp. 772–781, Oct. 1971.
[2] D. Middleton, "Canonical and quasi-canonical probability models of class a interference," *IEEE Trans. Electromagn. Compat.*, vol. EMC-25, no. 2, pp. 76–106, May 1983.
[3] W. J. Ebel and W. H. Tranter, "The performance of Reed–Solomon codes on a bursty-noise channel," *IEEE Trans. Commun.*, vol. 43, nos. 2–4, pp. 298–306, Feb. 1995.
[4] J. Ha and S. W. McLaughlin, "Low-density parity-check codes over Gaussian channels with erasures," *IEEE Trans. Inf. Theory*, vol. 49, no. 7, pp. 1801–1809, Jul. 2003.
[5] K. Li, A. Kavčić, R. Venkataramani, and M. F. Erden, "Channels with both random errors and burst erasures: Capacities, LDPC code thresholds, and code performances," in *Proc. IEEE Int. Symp. Inf. Theory (ISIT)*, Austin, TX, USA, Jun. 2010, pp. 699–703.
[6] F. Peng, M. Yang, and W. E. Ryan, "Simplified eIRA code design and performance analysis for correlated Rayleigh fading channels," *IEEE Trans. Wireless Commun.*, vol. 5, no. 4, pp. 720–725, Apr. 2006.
[7] S.-Y. Chung, "On the construction of some capacity-approaching coding schemes," Ph.D. dissertation, MIT, Cambridge, MA, 2000.
[8] S.-Y. Chung, T. J. Richardson, and R. L. Urbanke, "Analysis of sum-product decoding of low-density parity-check codes using a Gaussian approximation," *IEEE Trans. Inf. Theory*, vol. 47, no. 2, pp. 657–670, Feb. 2001.
[9] L. Song, F. Alajaji, and T. Linder, "Capacity of burst noise-erasure channels with and without feedback and input cost," *IEEE Trans. Inf. Theory*, vol. 65, no. 1, pp. 276–291, Jan. 2019.
[10] P. Chen, L. Kong, Y. Fang, and L. Wang, "The design of protograph LDPC codes for 2-D magnetic recording channels," *IEEE Trans. Magn.*, vol. 51, no. 11, Nov. 2015, Art. no. 3101704.
[11] S. J. Johnson, "Burst erasure correcting LDPC codes," *IEEE Trans. Commun.*, vol. 57, no. 3, pp. 641–652, Mar. 2009.
[12] P. Melo, C. Pimentel, and F. Alajaji, "LDPC decoding over nonbinary queue-based burst noise channels," *IEEE Trans. Veh. Technol.*, vol. 65, no. 1, pp. 452–457, Jan. 2016.
[13] A. R. Krishnan, R. Radhakrishnan, B. Vasić, A. Kavcic, W. Ryan, and F. Erden, "2-D magnetic recording: Read channel modeling and detection," *IEEE Trans. Magn.*, vol. 45, no. 10, pp. 3830–3836, Oct. 2009.
[14] D. Blackwell, L. Brieman, and A. J. Thomasian, "Proof of Shannon's transmission theorem for finite-state indecomposable channels," *Ann. Math. Stat.*, vol. 29, no. 4, pp. 1209–1220, Dec. 1958.
[15] E. N. Gilbert, "Capacity of a burst-noise channel," *Bell Syst. Tech. J.*, vol. 39, pp. 1253–1266, Sep. 1960.
[16] E. O. Elliott, "Estimates of error rates for codes on burst-noise channels," *Bell Syst. Tech. J.*, vol. 42, pp. 1977–1997, Sep. 1963.
[17] M. Mushkin and I. Bar-David, "Capacity and coding for the Gilbert-Elliott channels," *IEEE Trans. Inf. Theory*, vol. 35, no. 6, pp. 1277–1288, Nov. 1989.
[18] E. Martinian and C.-E. W. Sundberg, "Burst erasure correction codes with low decoding delay," *IEEE Trans. Inf. Theory*, vol. 50, no. 10, pp. 2494–2502, Oct. 2004.
[19] P. Sadeghi, R. A. Kennedy, P. B. Rapajic, and R. Shams, "Finite-state Markov modeling of fading channels—A survey of principles and applications," *IEEE Signal Process. Mag.*, vol. 25, no. 5, pp. 57–80, Sep. 2008.
[20] A. Badr, A. Khisti, W. T. Tan, and J. Apostolopoulos, "Streaming codes with partial recovery over channels with burst and isolated erasures," *IEEE J. Sel. Topics Signal Process.*, vol. 9, no. 3, pp. 501–516, Apr. 2015.
[21] W. E. Ryan and S. Lin, *Channel Codes: Classical and Modern*. Cambridge, U.K.: Cambridge Univ. Press, 2009.
[22] J. Li, S. Lin, K. Abdel-Ghaffar, W. E. Ryan, and D. J. Costello, "Globally coupled LDPC codes," in *Proc. Inf. Theory Appl. Workshop (ITA)*, La Jolla, CA, USA, Jan. 2016, pp. 1–10.
[23] J. Li, S. Lin, K. Abdel-Ghaffar, W. E. Ryan, and D. J. Costello, *LDPC Code Designs, Constructions, and Unification*. Cambridge U.K.: Cambridge Univ. Press, 2017.
[24] J. Li, K. Liu, S. Lin, and K. Abdel-Ghaffar, "Reed–Solomon based globally coupled quasi-cyclic LDPC codes," in *Proc. Inf. Theory Appl. Workshop (ITA)*, San Diego, CA, USA, Feb. 2017, pp. 1–10.
[25] J. Li, K. Liu, S. Lin, and K. Abdel-Ghaffar, "Reed–Solomon based non-binary globally coupled LDPC codes: Correction of random errors and bursts of erasures," in *Proc. IEEE Int. Symp. Inf. Theory (ISIT)*, Aachen, Germany, Jun. 2017, pp. 381–385.
[26] Y.-C. Liao, H.-C. Chang, and S. Lin, "Generalized globally-coupled low-density parity-check codes," in *Proc. IEEE Inf. Theory Workshop (ITW)*, Guangzhou, China, Nov. 2018, pp. 1–5.
[27] Y.-C. Liao, H.-C. Chang, and S. Lin, "Scalable globally-coupled low-density parity check-codes," in *Proc. IEEE Int. Symp. Turbo Codes Iterative Inf. Process. (ISTC)*, Hong Kong, Dec. 2018, pp. 1–5.
[28] J. Zhang, B. Bai, X. Mu, H. Xu, Z. Liu, and H. Li, "Construction and decoding of rate-compatible globally coupled LDPC codes," *Wireless Commun. Mobile Comput.*, vol. 2018, May 2018, Art. no. 4397671.
[29] Y.-C. Liao, C. Lin, H.-C. Chang, and S. Lin, "A (21150, 19050) GC-LDPC decoder for NAND flash applications," *IEEE Trans. Circuits Syst. I, Reg. Papers*, vol. 66, no. 3, pp. 1219–1230, Mar. 2019.
[30] W. Zhou, L. Cheng, and L. Zhang, "Construction of replacement set in the GC-LDPC codes based on BIBDs," in *Proc. Veh. Technol. Conf. (VTC-Spring)*, Kuala Lumpur, Malaysia, Apr. 2019, pp. 1–5.
[31] P. Parag, J. Chamberland, H. D. Pfister, and K. Narayanan, "Code-rate selection, queueing behavior, and the correlated erasure channel," *IEEE Trans. Inf. Theory*, vol. 59, no. 1, pp. 397–407, Jan. 2013.
[32] A. Ashikhmin, G. Kramer, and S. ten Brink, "Extrinsic information transfer functions: Model and erasure channel properties," *IEEE Trans. Inf. Theory*, vol. 50, no. 11, pp. 2657–2673, Nov. 2004.
[33] E. Sharon, A. Ashikhmin, and S. Litsyn, "EXIT functions for binary input memoryless symmetric channels," *IEEE Trans. Commun.*, vol. 54, no. 7, pp. 1207–1214, Jul. 2006.
[34] G. Liva and M. Chiani, "Protograph LDPC codes design based on EXIT analysis," in *Proc. IEEE Global Commun. Conf. (GLOBECOM)*, Washington, DC, USA, Nov. 2007, pp. 3250–3254.
[35] J. Thorpe, "Low-density parity-check (LDPC) codes constructed from protographs," Jet Propuls. Lab., Pasadena, CA, USA, INP Prog. Rep. 42-154, Aug. 2003.
[36] D. G. M. Mitchell, M. Lentmaier, and D. J. Costello, "Spatially coupled LDPC codes constructed from protographs," *IEEE Trans. Inf. Theory*, vol. 61, no. 9, pp. 4866–4889, Sep. 2015.
[37] R. A. Horn and C. R. Johnson, *Matrix Analysis*. Cambridge, U.K.: Cambridge Univ. Press, 2012.
[38] S. Lin and D. J. Costello, *Error Control Coding: Fundamentals and Applications*, 2nd ed. Upper Saddle River, NJ, USA: Prentice-Hall, 2004.
[39] S. ten Brink, "Convergence behavior of iteratively decoded parallel concatenated codes," *IEEE Trans. Commun.*, vol. 49, no. 10, pp. 1727–1737, Oct. 2001.
[40] S. ten Brink, G. Kramer, and A. Ashikhmin, "Design of low-density parity-check codes for modulation and detection," *IEEE Trans. Commun.*, vol. 52, no. 4, pp. 670–678, Apr. 2004.

[41] T. J. Richardson, M. A. Shokrollahi, and R. L. Urbanke, "Design of capacity-approaching irregular low-density parity-check codes," *IEEE Trans. Inf. Theory*, vol. 47, no. 2, pp. 619–637, Feb. 2001.
[42] T. J. Richardson and R. L. Urbanke, *Modern Coding Theory*. Cambridge, U.K.: Cambridge Univ. Press, 2008.
[43] J. Chen and M. P. C. Fossorier, "Near optimum universal belief propagation based decoding of low-density parity check codes," *IEEE Trans. Inf. Theory*, vol. 50, no. 3, pp. 406–414, Mar. 2002.
[44] E. Pisek, D. Rajan, and J. R. Cleveland, "Trellis-based QC-LDPC convolutional codes enabling low power decoders," *IEEE Trans. Commun.*, vol. 63, no. 6, pp. 1939–1951, Jun. 2015.
[45] *Digital Video Broadcasting (DVB); Second Generation Framing Structure, Channel Coding and Modulation Systems for Broadcasting, Interactive Services, News Gathering and Other Broadband Satellite Applications*, Standard EN 302.307-1, ETSI, Nov. 2014.

JI ZHANG received the B.S. and M.S. degrees from the School of Information Engineering, Henan University of Science and Technology, China, in 2005 and 2010, respectively. He is currently pursuing the Ph.D. degree in communication and information system with the State Key Laboratory of Integrated Services Networks (ISN), Xidian University, China. His research interests include information and coding theory, and wireless communications.

BAOMING BAI (S'98–M'00–SM'18) received the B.S. degree from the Northwest Telecommunications Engineering Institute, China, in 1987, and the M.S. and Ph.D. degrees in communication engineering from Xidian University, China, in 1990 and 2000, respectively. From 2000 to 2003, he was a Senior Research Assistant with the Department of Electronic Engineering, City University of Hong Kong. Since April 2003, he has been with the State Key Laboratory of Integrated Services Networks (ISN), School of Telecommunication Engineering, Xidian University, China, where he is currently a Professor. In 2005, he was with the University of California, Davis, as a Visiting Scholar. His research interests include information theory and channel coding, wireless communication, and quantum communication.

MIN ZHU (S'15–M'17) received the B.S., M.S., and Ph.D. degrees in communication and information system from Xidian University, China, in 2006, 2009, and 2016, respectively. From 2014 to 2015, she was with the Department of Electronic Engineering, University of Notre Dame, Notre Dame, IN, USA, as a Visiting Ph.D. Student. She is currently with the State Key Laboratory of Integrated Services Networks (ISN), Xidian University. Her research interests include channel coding and their applications to communication systems.

SHUANGYANG LI received the B.S. and M.S. degrees from Xidian University, China, in 2013 and 2016, respectively, where he is currently pursuing the Ph.D. degree with the State Key Laboratory of Integrated Services Networks (ISN), School of Telecommunication Engineering. His research interests include signal processing, channel coding, and their applications to communication systems.

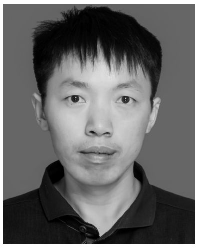

HUAAN LI received the B.S. degree in electrical and information engineering from the Harbin Institute of Technology, Harbin, China, in 2013, and the M.S. degree in signal and information processing from Lanzhou University, Lanzhou, China, in 2016. He is currently pursuing the Ph.D. degree in communication and information system with the State Key Laboratory of Integrated Services Networks (ISN), Xidian University, China. His research interests include information and coding theory, and wireless communications.